
Compositional Models for Estimating Causal Effects

Purva Pruthi David Jensen

College of Information and Computer Sciences,
 University of Massachusetts Amherst
 {ppruthi, jensen}@cs.umass.edu

Abstract

Many real-world systems can be usefully represented as sets of interacting components. Examples include computational systems, such as query processors and compilers; natural systems, such as cells and ecosystems; and social systems, such as families and workgroups. However, current approaches to estimating *potential outcomes* and *causal effects* typically treat such systems as single units, represent them with a fixed set of variables, and assume a homogeneous data-generating process. In this work, we study a *compositional* approach for estimating individual-level potential outcomes and causal effects in structured systems, where each unit is represented by an *instance-specific* composition of multiple heterogeneous components. The compositional approach decomposes unit-level causal queries into more fine-grained queries, explicitly modeling how unit-level interventions affect component-level outcomes to generate a unit’s outcome. We demonstrate this approach using modular neural network architectures and show that it provides benefits for causal effect estimation from observational data, such as accurate causal effect estimation for structured units, increased sample efficiency, improved overlap between treatment and control groups, and compositional generalization to units with unseen combinations of components. Remarkably, our results show that compositional modeling can improve the accuracy of causal estimation even when component-level outcomes are unobserved. We also create and use a set of real-world evaluation environments for the empirical evaluation of compositional approaches for causal effect estimation and demonstrate the role of composition structure, varying amounts of component-level data access, and component heterogeneity in the performance of compositional models as compared to the non-compositional approaches.

1 Introduction

Many real-world systems are *heterogeneous* and *modular*—they decompose into heterogeneous functional *components* that interact to produce system behavior [Callebaut and Rasskin-Gutman, 2005, Johansson et al., 2022]. In addition, many applications require estimating individual-level potential outcomes and treatment effects, including personalized medicine [Curth et al., 2024], individualized instruction [Kochmar et al., 2022], and custom online advertising [Bottou et al., 2013]. Estimating individual treatment effects for compositional systems is an important problem, particularly as the complexity of modern technological systems increases. Modern computational systems such as databases, compilers, and multi-agent systems usually generate large amounts of experimental and observational data containing fine-grained information about the structure and behavior of modular systems, which often remains unused by the existing approaches for estimating causal effects.

Figure 1 provides a schematic overview of causal inference for compositional systems and how it is addressed by different approaches to causal estimation. Consider a relational database query execution system with component operations such as `scan`, `sort`, `aggregate`, and `join`. The system takes in-

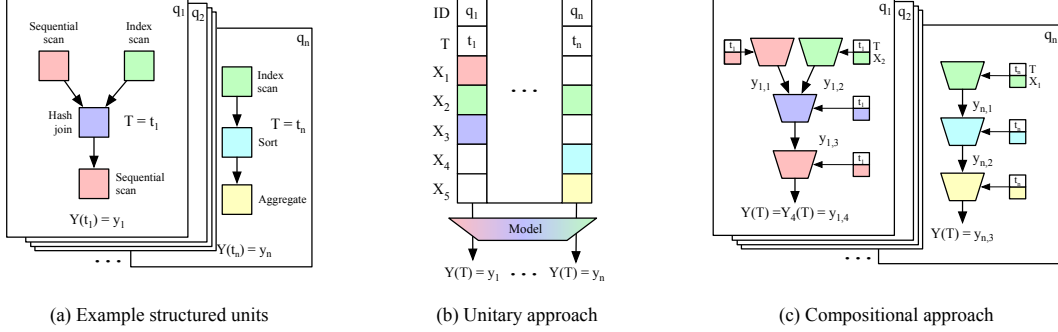


Figure 1: **Overview of key ideas:** (a) **Structured units:** Examples of units composed of multiple heterogeneous components. Each color represents a distinct component. Treatment T is applied to the unit, and the compositional system processes the inputs under intervention, returning potential outcomes. (b) **Unitary approach:** The standard approach for effect estimation flattens the underlying structure. It uses a fixed-size representation for each unit, aggregating component-level information to estimate unit-level potential outcomes. (c) **Compositional approach:** The compositional approach models each unit with an instance-specific structure. Component-level covariates X_j and outcomes Y_j are used to train each component model, and component-level outcomes are hierarchically aggregated to estimate unit-level potential outcomes. Each color represents a distinct component model with different parameters.

put including tables (e.g., A, B) and a query execution plan (e.g., `scan(join(scan(A), scan(B)))`) and returns a new table as output. Query executions represent the unit of analysis, and query plans explicitly describe the *compositional* and *hierarchical* structure of those units — query executions consist of heterogeneous component operations that can be combined in a vast number of different ways. In addition, the compositional structure of query execution is *instance-specific* — the number, kind, and structure among components may differ across each unit. These units can be represented as hierarchical graphs (e.g., parse-trees), where each node is a component operation and edges represent the information flow between the components.

Given such a system, consider modeling the causal effect of memory size on execution time for different query plans. This problem can be formulated as using observational data to estimate the *individual-level* effects of interventions on structured units.¹ In real-world data on query execution, interventions such as memory size might be chosen based on the structure and features of the query, making the data *observational*. In the terminology of causal inference, each query execution is a *unit of analysis*, the features of the relations are *pre-treatment covariates*, memory size is the *intervention*, and execution time is the *potential outcome* [Rubin, 1974, 2005]. We might also want to predict the effects for a population of arbitrary query executions that contain novel combinations of the component operations. In that case, it is desirable for the learned models to *compositionally generalize* to units with unseen combinations of the components. Other real-world use-cases of causal reasoning in structured data are discussed in the supplementary material (Section B).

Standard approaches to heterogeneous treatment effect estimation [e.g., Hill, 2011, Athey and Imbens, 2016, Wager and Athey, 2018, Chernozhukov et al., 2018] typically ignore the underlying structure of the data-generating process and represent each unit using a fixed-size feature representation, assuming a homogeneous data-generating process [Holland, 1986]. However, using fixed-size representation for compositional units poses several estimation challenges. As the structure and complexity of each unit vary, estimating effects at the unit level requires reasoning about the similarity among the heterogeneous units in high-dimensional space, and representing all the units with the same features leads to sparse feature representation and aggregation of the features of multiple instances of each component. We use the term *unitary models* to denote these approaches that exclusively model unit-level quantities.

In contrast, we study a *compositional* approach to causal effect estimation for structured units from observational data. This approach facilitates construction of *instance-specific* causal models (models

¹Here, individual-level effect estimation refers to conditional average treatment effect (CATE) estimation and heterogeneous treatment effect estimation [Athey and Imbens, 2016, Shalit et al., 2017, Künnel et al., 2019].

whose structure changes based on the specific components present in the specific units being modeled) using *modular* neural network architectures to explicitly represent the components of each unit of analysis (Figure 1(c)).² **We formalize a novel compositional framework in the context of causal effects and potential outcomes** to facilitate the study of the compositional approach and provide a detailed analysis of the unique benefits and costs of such an approach for accurate unit-level CATE estimation. We focus on the case of hierarchically structured compositional systems without feedback and with simple interactions because they represent the minimal compositional systems to understand the key characteristics of the compositional approach as compared to unitary modeling approaches.

We discover that the compositional approach provides several novel benefits for causal inference from observational data. The instance-specific model allows *scalable* causal effect estimation for variable-size units by greatly reducing the inherent dimensionality of the task. Instance-specific modular architectures are widely used in associational machine learning for modeling large-scale natural language data, structured vision data, and sequential decision-making, providing sample efficiency and computation benefits [Shazeer et al., 2016, Pfeiffer et al., 2023]. However, only a relatively sparse body of work in causal inference has focused on using instance-specific modular models using hierarchical and relational data [Maier et al., 2013, Lee and Honavar, 2016, Salimi et al., 2020, Ahsan et al., 2023], and even this work has been severely hampered by the lack of available data from compositional domains. To address this gap, **we introduce three novel and realistic evaluation environments to evaluate compositional approaches for causal effect estimation** — query execution in relational databases, matrix processing on different types of computer hardware, and simulated manufacturing assembly line data based on a realistic simulator.

The modular structure incorporated in the compositional approach facilitates effect estimation for units with unseen combinations of components, enabling *compositional generalization*. In various fields of machine learning — computer vision [Andreas et al., 2016], language [Hupkes et al., 2020], reinforcement learning [Peng et al., 2019], and program synthesis [Shi et al., 2024], researchers have studied the compositional generalization capabilities of the modular approaches as compared to non-modular approaches for prediction tasks [Bahdanau et al., 2019, Jarvis et al., 2023, Schug et al., 2024]. However, a study of the benefits of the compositional approach compared to the standard approaches is missing in causal inference. **We study the relative compositional generalization capabilities of compositional and unitary approaches in estimating individual treatment effects for novel units.**

Individual effect estimation from observational data requires assumptions such as *ignorability* and *overlap* [Pearl, 2009, Rubin, 2005]. Satisfying the overlap assumption becomes challenging as the dimensionality of covariates increases [D’Amour et al., 2021]. Learning lower-dimensional representations of data that satisfies the ignorability and overlap assumption is desirable in such situations [Johansson et al., 2016, 2022]. Exploiting the compositionality of the underlying data-generating process is one of the ways to learn lower dimensional representation, allowing better overlap between treatment groups. **We show that the compositional approach performs better as the distributional mismatch between the treatment and control groups increases, especially in cases where treatment is assigned based on the unit’s structure.**

Despite these potential benefits, learning compositional models for effect estimation has pitfalls, including larger numbers of parameters to estimate, sensitivity to individual components, and errors in modeling component interactions. In this paper, **we analyze the role of component-level data access, composition structure, and heterogeneity in component function complexity in the relative performance of the compositional approach**. For example, we observe that compositional and unitary approaches perform similarly when modeling systems with homogeneous component functions—such as matrix processing—where a single component (e.g., matrix multiplication) dominates the overall unit-level outcome and all component outcome functions belong to the same polynomial class. See Section 5 for additional pitfalls.

²Modular neural network architectures are chosen as an implementation choice to demonstrate compositional approach but component-wise causal estimation can be done using a variety of parametric and non-parametric model classes.

2 Compositional Framework for Causal Effect Estimation

Below, we describe the compositional data-generating process in modular systems, provide the estimands of interest at the unit and component levels, and discuss identifiability assumptions.

Preliminaries: Assume that each unit i has pre-treatment covariates $\mathbf{X}_i = \mathbf{x} \in \mathcal{X} \subset \mathbb{R}^d$, a binary treatment $T_i \in \{0, 1\}$, and two potential outcomes $\{Y_i(0), Y_i(1)\} \in \mathcal{Y} \subset \mathbb{R}$ [Rubin, 1974, 2005]. In observational data, we only observe one of the potential outcomes for each unit, $Y_i = Y_i(T_i)$, known as the *observed* or *factual* outcome. The missing outcomes $Y_{iCF} = Y_i(1 - T_i)$ are known as *unobserved* or *counterfactual* outcomes. Conditional average treatment effect (CATE) is defined as $\tau(x) : \mathbb{E}[Y_i(1) - Y_i(0) | \mathbf{X}_i = \mathbf{x}]$. Estimating CATE requires assumptions of ignorability, overlap, and consistency [Rosenbaum and Rubin, 1983]. Under these assumptions, $\tau(x)$ is identifiable by $\tau(\mathbf{x}) = \mathbb{E}[Y_i | \mathbf{X}_i = \mathbf{x}, T = 1] - \mathbb{E}[Y_i | \mathbf{X}_i = \mathbf{x}, T = 0]$ [Pearl, 2009]. CATE estimation typically uses direct outcome modeling with treatment as a feature, separate regression models [Künzel et al., 2019], or propensity score methods [Kennedy, 2023]. We illustrate the compositional approach by directly estimating the potential outcomes using shared treatment.

2.1 Compositional data generating process

Consider a compositional system with k distinct and heterogeneous classes of components: $\mathcal{M} = \{M_1, M_2, \dots, M_k\}$. All units share this set of reusable components. Each structured unit $Q_i : (G_i, \{\mathbf{X}_{ij}\}_{j=1:m_i})$ is described using an interaction graph G_i and a set of component-specific covariates $\{\mathbf{X}_{ij}\}_{j=1:m_i}$, where m_i denotes the number of components in unit i . Note that the number of components m_i can be greater than the number of distinct components k in the system, indicating the presence of multiple instances of each component class in some or all units.

The graph $G_i = (C_i, E_i)$ is a directed hierarchical tree representing component interactions (Figure 1(a)), with nodes C_i and edges E_i . Each unit i contains components $C_i = \{c_1, c_2, \dots, c_{m_i}\}$, where each component belongs to a class $c \in M_o, o \in \{1, 2, \dots, k\}$. G_i defines the processing order of m_i components for unit i , with instance-specific structure varying across units. Components process structured units from top-to-bottom, with final output from the bottom-most node. For an edge $c_j \rightarrow c_{j'}$, c_j is the parent and $c_{j'}$ the child component. $Pa_{G_i}(c_{j'})$ denotes indices of components with direct edges to $c_{j'}$. Component j 's covariates are $\mathbf{X}_{ij} \in \mathbb{R}^{d_j}$, where subscript i denotes the unit and j denotes the component instance.

Shared treatment and treatment assignment mechanism in structured units: A unit-level treatment T_i is selected for each unit, affecting the potential outcomes of some or all components through shared or distinct mechanisms. While the compositional framework allows component-specific treatment analysis, we focus on unit-level treatments to facilitate a direct comparison of the compositional and unitary approaches. The treatment assignment mechanism $P(T_i = 1 | Q_i = q)$ depends on both the graph structure and joint covariate distribution, introducing two sources of observational bias: (1) distribution shift among the covariates; and (2) distribution shift in the structure and composition of the components between treatment groups.

Unit-level outcome and fine-grained outcomes: Let $Y_i(t)$ denote the unit-level and $\{Y_{ij}(t)\}_{j=1:m_i}$ denote the component-level potential outcomes under treatment t for unit Q_i . The interaction graph G_i also defines the causal dependencies among potential outcomes. We make the causal Markov assumption for components in the graph G_i that the potential outcome of a component j directly depends on the component's covariates \mathbf{X}_{ij} , shared treatment T_i and the outcomes from the parent components. For component class $o \in \{1, 2, \dots, k\}$, let μ_{ot} denote the ground-truth *expected* potential outcome function, shared across instances of the same component. If component-level noise is assumed to be zero-mean random variables $\epsilon_o(0), \epsilon_o(1)$ and $c_j \in M_o$,³ the data-generating process for $Y_{ij}(t), j \in \{1, 2, \dots, m_i\}$ and $t \in \{0, 1\}$:

$$Y_{ij}(t) = \mu_{ot}(\mathbf{X}_{ij}, \{Y_{il}(t)\}_{l \in Pa(c_j)}) + \epsilon_{io}(t). \quad (1)$$

The unit-level potential outcome is generated by aggregating component outcomes via an instance-specific function g : $Y_i(t) = g(Y_{i1}(t), Y_{i2}(t) \dots Y_{im_i}(t), G_i)$. For composition in the hierarchical

³Additive noise simplifies modeling conditional distributions of component potential outcomes in Section J.1, though the compositional approach extends to non-additive noise.

graph, the data-generating process of each component’s outcome already takes the input from the parent’s outcome, following Markov dependence (Equation 1). We can define these outcomes cumulatively, meaning we aggregate them up as we go along, so that the final component’s outcome represents the complete unit-level outcome, $Y_i(t) = Y_{im_i}(t)$, where m_i indicates the last component in G_i . For example, consider query execution time: rather than measuring each component’s time separately, we can measure the accumulated time of each component and all its parent components. In Figure 1(c), this cumulative approach means we can use the final sequential scan’s outcome for Q_1 as the total execution time of the unit. This formulation allows us to learn the instance-specific aggregation functions and unit outcomes as part of learning the component potential outcomes.

2.2 Unitary representation of compositional data

As already mentioned, an alternative to a compositional model is a unitary model in which units are represented by a single, fixed-size, high-dimensional feature vector, $\mathbf{X}_i \in \mathbb{R}^d$ that represents the aggregation of the component level input features $\{\mathbf{X}_{ij}\}_{j=1}^{m_i}$. For simplicity in our experiments, we assume the mean aggregation function and i.e., if there are N_o occurrences of component class o in unit i , then $\mathbf{X}_{io} = \frac{1}{N_o} \sum_{j, c_j \in M_o} \mathbf{X}_{ij}$. Similarly, corresponding outcomes are also aggregated. To fairly compare the unitary and compositional approaches, we also incorporate structural information by including the number of instances of each component N_{jl} present in each unit at each tree depth with maximum depth L : $\mathbf{X} = [\mathbf{X}_1, \mathbf{X}_2, \dots, \mathbf{X}_k, N_{11}, N_{12}, \dots, N_{kL}]$.

2.3 Causal Estimands

The CATE for a structured unit q is conditional on both the structure G_i and the set of component-level features $\{\mathbf{x}_{ij}\}_{j=1:m_i}$. Taking the conditional expectation with respect to the structure and variable-length representation of the units allows a more accurate definition of the CATE for compositional units than the standard unitary representation. For ease of notation to describe conditional distributions, we denote the combined inputs to a component j as $\mathbf{Z}_j(t) = (\mathbf{X}_j, \{Y_l(t)\}_{l \in Pa(C_j)})$.

Definition 2.1. *The conditional-average treatment effect (CATE) estimand for structured input $Q_i = q$ is defined as: $\tau(q) = \mathbb{E}[Y_i(1) - Y_i(0)|Q_i = q] = \mathbb{E}[Y_i(1) - Y_i(0)|Q_i = (G_i, \{\mathbf{x}_{ij}\}_{j=1:m_i})]$*

Definition 2.2. *The conditional-average treatment effect (CATE) estimand for component j with $\mathbf{X}_j = \mathbf{x}_j \in \mathbb{R}^{d_j}$ is defined as: $\tau(\mathbf{z}_j) = \mathbb{E}[Y_j(1) - Y_j(0)|\mathbf{Z}_j = \mathbf{z}_j]$.*

We define the component-wise distributions as $P(Y_j(t)|\mathbf{Z}_j(t) = \mathbf{z}_j)$. In hierarchical composition, the unit outcome equals the final component outcome: $\mathbb{E}[Y_i(t)|Q_i = q] = \mathbb{E}[Y_{im_i}(t)|Q_i = q]$. This conditional expectation can be expressed by marginalizing intermediate component outcomes using the Markov assumption (Equation 1).

$$\mathbb{E}[Y_i(t)|Q_i = q] = \int_{Y_{im_i-1}(t)} \int_{Y_{im_i-2}(t)} \cdots \int_{Y_{i1}(t)} \mathbb{E}[Y_{im_i}(t)|\mathbf{Z}_{im_i}(t)] \prod_{j=1}^{m_i-1} P(Y_{ij}(t)|\mathbf{Z}_{ij}(t))$$

We use the following nested expectation expression as shorthand for marginalization over intermediate component outcomes: $\mathbb{E}[Y_i(t)|Q_i = q] = \mathbb{E}_{Y_{i1:im_i-1}(t)} [\mathbb{E}[Y_{im_i}(t)|\mathbf{Z}_{im_i}(t)]]$

2.4 Identifiability assumptions

The key identifiability assumptions for component-level causal estimands are similar to those for unit-level estimands — ignorability, consistency, and overlap. However, in structured units having multiple heterogeneous components and instance-specific composition, it is more plausible for these assumptions to hold for the component level rather than the unit level, particularly for ignorability and overlap.

Ignorability: Component-level ignorability assumes that component level potential and assigned treatment are independent conditioned on the components’ covariates, i.e., $Y_j(1), Y_j(0) \perp T|\mathbf{X}_j$. Component-level ignorability is based on the intuition that components are distinct heterogeneous subsystems that are specialized to process parts of the whole input. This suggests that a subset of the unit-level high-dimensional covariates is sufficient to predict a component’s outcome, even when treatment might have been assigned based on the structure of the components or joint distribution of the component covariates. The component-level potential outcomes depend on both the component’s pre-treatment covariates and the potential outcomes of the parent components. As the treatment is assigned

before any component’s potential outcomes are observed, we can assume that the component’s covariates \mathbf{X}_j are sufficient to satisfy ignorability assumptions.

Overlap: Component-level overlap assumes that overlap holds for the component level covariates $\mathbf{X}_j = \mathbf{x}_j$, i.e., $\forall \mathbf{x}_j \in \mathcal{X}_j, t \in \{0, 1\} : 0 < p(T = t | \mathbf{X}_j = \mathbf{x}_j) < 1$. When unit-level overlap holds, component-level overlap is implied automatically for the feature subset. In compositional data, there can be two sources for distribution mismatch. (1) *Structure-based treatment assignment*: Suppose treatment depends strongly on graph structure ($P(T = 1 | G = g_1) = 1, P(T = 1 | G = g_2) = 0$). For unitary representation including structural features N_{jl} , the overlap assumption is violated for units with the structures as g_1 and g_2 , while overlap is maintained for compositional approaches as the structure is incorporated as part of the model rather than input representation. If we exclude structural information from unitary representation, then overlap is satisfied, but ignorability is violated because the structure is a confounder affecting both T_i and Y_i . (2) *Covariate-based treatment assignment*: When treatment depends on the covariate distribution, both approaches’ identifiability relies on overlap quality. Due to the compositional nature of units, violation of overlap for a component’s covariates violates overlap for the unit-level and vice versa. However, due to the lower dimensionality of the component’s covariates, the degree of distribution mismatch between the covariates is likely to be lower than the unit-level high-dimensional covariates.

Identifiability for hierarchical composition: The CATE estimand for a structured unit $Q_i = q$ is identified by the following: $\tau(q) = \mathbb{E}_{Y_{1:m_i-1}}[\mathbb{E}[Y_{m_i} | \mathbf{Z}_{m_i} = \mathbf{z}_{m_i}, T = 1]] - \mathbb{E}_{Y_{1:m_i-1}}[\mathbb{E}[Y_{m_i} | \mathbf{Z}_{m_i} = \mathbf{z}_{m_i}, T = 0]]$ if we assume Markov dependence assumption (Equation 1), component-wise ignorability, overlap, and consistency. The proof is provided in the supplementary material.

Additive parallel composition (special case): A special case of the interaction graph G_i is when all the components are parallel and independently compute the potential outcomes. This condition can be expressed as when the potential outcomes of components are *conditionally independent* given the component’s covariates, i.e., $Y_j(t) \perp Y_l(t) | \mathbf{X}_j \forall j \in \{1, \dots, k\}, j \neq l$. Suppose the aggregation function is a linear combination of the component’s outcomes, e.g., addition. The unit-level CATE can be expressed as the sum of the potential outcome estimands. $Y_{ij}(t) = \mu_{ot}(\mathbf{X}_{ij}) + \epsilon_{io}(t), Y_i(t) = \sum_{j=1}^{m_i} Y_{ij}(t)$. In that case, the CATE can be directly expressed as the linear combination of the component-level CATE and is identified as follows: $\tau(q) = \sum_{j=1}^{m_i} \tau(\mathbf{x}_{ij}) = \sum_{j=1}^{m_i} \mathbb{E}[Y_{ij} | \mathbf{x}_{ij}, T_i = 1] - \mathbb{E}[Y_{ij} | \mathbf{x}_{ij}, T_i = 0]$. The proof is provided in the supplementary material. Parallel composition appears across machine learning domains—from independent composition of latent object attributes in computer vision [Higgins et al., 2018, Wiedemer et al., 2024] to spatial skill composition in reinforcement learning [Van Niekerk et al., 2019]. Similarly, sequential composition appears in the options framework in reinforcement learning [Sutton et al., 1999]. Our work examines these varied composition structures to understand their impact on compositional generalization.

3 Learning compositional models from observational data

Below, we discuss algorithms for learning the hierarchical composition model from observational data, given different amounts of information about the component’s covariates and outcomes. We include additional details about modeling component-wise distributions and parallel composition models in the supplementary material (Section J).

3.1 Hierarchical Composition Model

Model Training: The component models for estimating component-level potential outcomes are denoted by $\hat{f}_{\theta_o} : \mathbb{R}^{d_o} \times \mathbb{R}^D \times \{0, 1\} \rightarrow \mathbb{R}$, $o \in \{1, 2, \dots, k\}$, assuming maximum in-degree of the graph G_i as D . Each model corresponding to component class o is parameterized by separate parameters θ_o . For a given observational data set with n samples, $\mathcal{D}_F = \{q_i, t_i, y_i\}_{i=1:n}$, we assume that we observe component-level features $\{\mathbf{x}_{ij}\}_{j=1:m_i}$, assigned treatment t_i and fine-grained component-level potential outcomes $\{y_{ij}\}_{j=1:m_i}$ along with unit-level potential outcomes y_i . If component instance $c_j \in M_o$, training of each component model o involves the independent learning of the parameters by minimizing empirical risk: $\theta_o^* := \arg \min_{\theta_o} \frac{1}{N_o} \sum_{m=1}^{N_o} (\hat{f}_{\theta_o}(\mathbf{z}_m, t_m) - y_m)^2$, where N_o denotes the total number of component instances of component class o across all the N samples. The potential outcome of each component is computed using input features of that component, shared unit-level treatment, and *observed* potential outcomes of the parent’s component.

Model Inference: To estimate CATE for a unit i , a modular architecture consisting of m_i component models is instantiated with the same input and output structure as G_i (Figure 1(c)). During inference for treatment $T = t$, the predictions of potential outcomes of the parent’s components $\{\hat{y}_{lt}\}_{l \in Pa(c_j)}$ are passed as an input to estimate the conditional distribution of the outcome $\hat{y}_{jt} = \hat{f}_{\theta_o^*}(\mathbf{x}_j, \{\hat{y}_{lt}\}_{l \in Pa(c_j)}, t) = \hat{f}_{\theta_o^*}(\hat{z}_{jt}, t)$. The estimate of CATE is obtained by taking the difference between the estimates of the last component instance $c_{m_i} \in M_o$: $\hat{\tau}(q) = \hat{f}_{\theta_o^*}(\hat{z}_{m_i1}, 1) - \hat{f}_{\theta_o^*}(\hat{z}_{m_i0}, 0)$.

3.2 Relaxing assumptions about component-level data access

The model description above assumes observed component-level covariates and outcomes. This assumption is often reasonable, given the wide availability of fine-grained data for many structured domains. However, other cases exist when only the unit-level covariates \mathbf{X} and outcomes are observed, and the component-level covariates \mathbf{X}_j and outcomes Y_j are unobserved. Below, we discuss hierarchical composition models for these cases.

Case 1: Unobserved \mathbf{X}_j , observed Y_j : We jointly learn the lower-dimensional component-level representations $\phi_o : \mathbb{R}^d \rightarrow \mathbb{R}^{d_o^*}$, as well as the parameters of outcome functions \hat{f}_{θ_o} : $\theta_o := \arg \min_{\theta} \frac{1}{N_o} \sum_{m=1}^{N_o} (\hat{f}_{\theta_o}(\phi_o(\mathbf{x}_m), \{y_l\}_{l \in Pa(c_m)}, t_m) - y_m)^2$. ϕ_o is jointly trained with the parameters θ_o , so that the relevant variables for predicting y_{ij} are selected.

Case 2: Observed \mathbf{X}_j , unobserved Y_j : The model architecture remains the same as before, but we do not have individual component-level loss functions and only know the loss function for unit-level outcomes. Due to this, the parameters of the components are jointly learned to optimize the loss of estimating unit-level outcomes. If \circ denotes the functional composition, and functions are composed in the same hierarchical order as G_i , then the joint loss function is given by: $[\theta_1, \theta_2 \dots \theta_k] := \arg \min_{\Theta} \frac{1}{N} \sum_{i=1}^N (\hat{f}_{\theta_{m_i}} \circ \hat{f}_{\theta_{m_i-1}} \circ \dots \circ \hat{f}_{\theta_1}(\mathbf{x}_{i1}, t_i) - y_i)^2$

Case 3: Unobserved \mathbf{X}_j and unobserved Y_j : In this case, we only assume the knowledge of G_i . $[\theta_1, \theta_2 \dots \theta_k] := \arg \min_{\Theta} \frac{1}{N} \sum_{i=1}^N (\hat{f}_{\theta_{m_i}} \circ \hat{f}_{\theta_{m_i-1}} \circ \dots \circ \hat{f}_{\theta_1}(\phi_1(\mathbf{x}_i), t_i) - y_i)^2$

4 Experimental Infrastructure

We describe the experimental setup to evaluate the models across various *in-distribution* and *out-of-distribution* settings, with details provided in the supplementary material (Section K)⁴.

4.1 Datasets

Research on modeling causal effects for compositional data has been hampered by the lack of real-world benchmarks. To facilitate effective empirical evaluation of the utility of compositional modeling of causal effect estimation, we introduce two benchmarks based on real-world computational systems and one benchmark based on a realistic simulation.

Query execution in relational databases: We collected real-world query execution plans data by running 10,000 publicly available SQL queries against the Stack Overflow database under different configurations (memory size, indexing, page cost), treating configuration parameters as interventions and execution time as the potential outcome, assuming additive composition.

Manufacturing plant data: We use a discrete-event simulation framework, Simpy, to generate realistic manufacturing plant data. The simulation includes four manufacturing processes (material processing, joining, electronics processing, and assembly) combined across 50 hierarchical manufacturing line layouts, assuming hierarchical composition. Each layout consists of various product demand (5-1,000) with different raw material inventories as covariates. Treatment compares five versus fifteen skilled workers, measuring total parts produced as outcomes.

Matrix operations processing: The dataset consists of 25,000 samples for 25 matrix expression structures (units) evaluated on two different computer hardware (treatment), with matrix dimensions ranging from 2 to 1,000. Component operations encompass 12 component operations (e.g., multiplication, inverse, singular value decomposition, etc.). We ensure each operation is executed

⁴Data and code for creating benchmarks and reproducing experiments will be provided upon publication.

individually, ensuring parallel composition with additive aggregation function. Matrix size is used as a biasing covariate to create a distribution mismatch between treatment groups.

Synthetic data: In addition to these real-world benchmarks, we also generate simulated data to systematically understand the role of component-level data access, composition structure, and heterogeneity in components’ response surfaces. Composition structures include sequential and additive parallel composition. Structured units are generated by sampling binary trees (max depth=10) with $k = 10$ heterogeneous modules, each having $d_j = 1$ feature ($d = 10$ features total).

4.2 Models and Evaluation Criteria

Compositional Models: We implement four versions of the compositional models (hierarchical and parallel, depending on the domain) with varying amount of component-level data access as discussed in Sections 3.1 and 3.2: (1) *Compositional (observed \mathbf{X}_j , observed Y_j)*; (2) *Compositional (unobserved \mathbf{X}_j , observed Y_j)*; (3) *Compositional (observed \mathbf{X}_j , unobserved Y_j)*; and (4) *Compositional (unobserved \mathbf{X}_j , unobserved Y_j)*. The component-level models are implemented as neural networks, independently trained in case of access to fine-grained outcomes and jointly end-to-end trained otherwise. **Note:** Unless stated explicitly, the legend “compositional” in experimental results implies a model with observed component-level covariates \mathbf{X}_j and outcomes Y_j .

Baselines: We compare the performance of the compositional models with three types of existing approaches for CATE estimation: (1) *TNet*, a neural network-based CATE estimator [Curth and Van der Schaar, 2021]; (2) *X-learner*, a meta learner that uses plug-in estimators to compute CATE, with random forest as the base model class [Künzel et al., 2019]; (3) Non-parametric *Double ML* [Chernozhukov et al., 2018]; and (4) *Vanilla neural network* and *random forest*-based outcome regression models.

Creation of observational data sets: Real-world computational systems provide experimental datasets with observed outcomes for both treatments, from which we create observational datasets by introducing structure and covariate-based confounding bias [Gentzel et al., 2021]. Bias strength ranges from 0 (experimental) to 10 (observational), with treatment probabilities varying between 0.01-0.99, creating treatment group distribution shifts. Unconfoundedness holds as biasing information is observed in both approaches. Higher “bias strength” indicates higher treatment probability for specific biasing covariate values and structure.

Evaluating compositional generalization: We evaluate compositional generalization by training on structures with 2 to K module combinations and testing on combinations containing all K module combinations. For example, when training on 2-module combinations, we use all possible pairs (e.g., (C_1, C_2) , (C_1, C_3) , (C_2, C_3)), including varied orders and repeated modules (e.g., (C_1, C_2, C_1)), and test on larger combinations like (C_1, C_2, C_3) . For real-world data, we train on structures with smaller tree depths and test on larger ones.

Performance and Evaluation Metrics: Performance is evaluated in two settings: *WID* (same structure/covariate distribution in train/test) and *OOD*, which includes (1) *compositional generalization* (testing on unseen component combinations) and (2) *observational bias* (structure/covariate-dependent treatment assignment). We measure PEHE loss [Hill, 2011]: $\epsilon_{PEHE}(\hat{f}) = \mathbb{E}[(\hat{\tau}_{\hat{f}}(q) - \tau(q))^2]$, and R^2 score for datasets with large outcome values or high performance variability.

5 Findings

In this section, we provide the key findings from our experiments and discuss the mechanisms responsible for compositional models’ performance compared to the baselines.

Compositional models can provide substantially more accurate CATE estimation for structured units: Figure 2(a) shows results from the manufacturing domain in which compositional and unitary models were learned from experimental data and evaluated in terms of their in-distribution performance. The compositional model has substantially lower error than the baselines, particularly for small sample sizes. More detailed analysis showed that the performance advantage of compositional models in this setting is primarily due to two factors: (1) units in this domain have heterogeneous hierarchical structure and instance-specific models more accurately represent this structure; and (2)

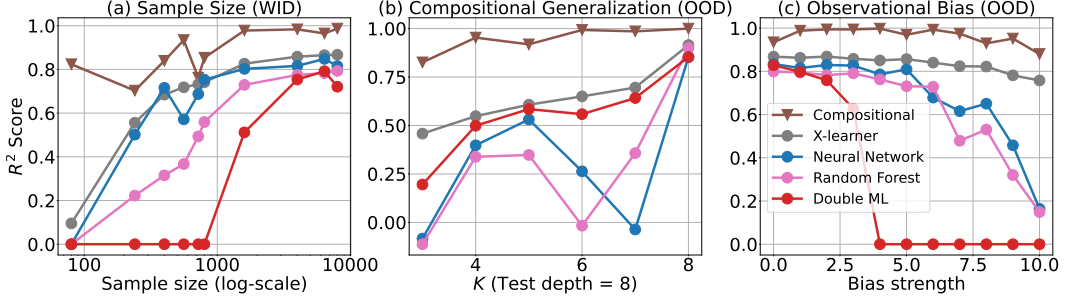


Figure 2: **Results on manufacturing domain** (10,000 samples). We report R^2 between CATE estimates and ground-truth effects (higher is better). (a) *Sample-size efficiency (WID)*: Compositional models are more accurate and sample-efficient in CATE estimation for within-distribution settings. (b) *Compositional generalization (OOD)*: Models are trained on units with tree depth $\leq K$ and evaluated on a test-set with depth 8. Compositional models generalize to the unseen combinations due to compositional structure whereas non-compositional baselines perform comparably only after training on units similar to test data. (c) *Effect of increasing observational bias (OOD)*: Models are trained and tested on data with increasing observational bias strength between assigned treatment and tree depth. Compositional models and X-learner are less affected by increased observational bias.

compositional models were learned with higher sample efficiency due to the existence of multiple samples of each component per unit (see Figure 6(a) in the supplementary materials).

Incorporating modular structure enables compositional generalization: Figures 2(b) and 3 report the compositional generalization performance of the models in the manufacturing and synthetic domains, respectively. Compositional models were able to successfully generalize to high-complexity units (large depth or number of module combinations, respectively) even though they had only been trained on low-complexity units. In contrast, unitary models perform worse (often *far* worse) until they are trained on units that equal or nearly equal the compositional complexity of the test units.

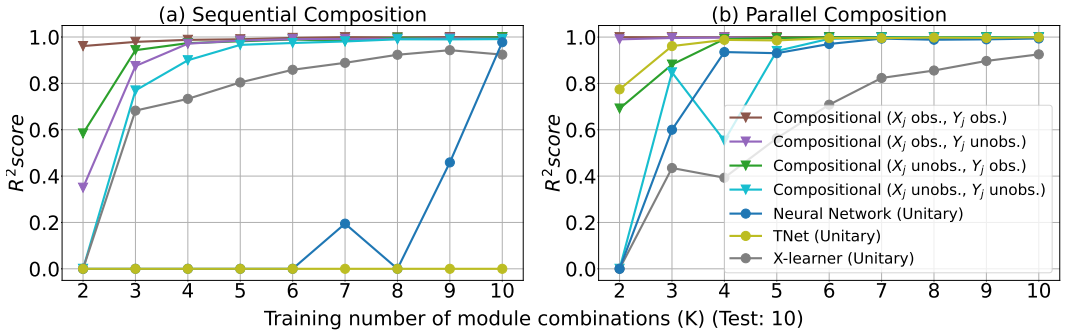


Figure 3: **Role of component-level data access and composition structure in the performance of compositional models:** R^2 score for models evaluated on compositional generalization task with varying degrees of component-level data access. (Higher is better; PEHE errors are reported in Figure 13 of the supplementary material). We observe that end-to-end trained models incorporating just modular structure compositionally generalize as trained on more module combinations. Unitary models show compositional generalization for additive parallel composition but perform comparably only for in-distribution combinations ($K=10$) for sequential composition, except X-learner. Note that the number of training samples increases as training depth increases.

Compositional models are less affected by observational bias in treatment assignment: Figure 2(c) reports the effects of differing degrees of observational bias based on the instance-specific structure in the manufacturing domain. Compositional models (and the unitary X-learner) are least affected by this form of observational bias. Other unitary models (Neural network and Random forest) are strongly affected, and another unitary model (double ML) is the most strongly affected due to its use of propensity score weighting. Figure 4(a) reports results for the query execution domain, where bias was introduced based on the covariate distribution. The error of all models increases

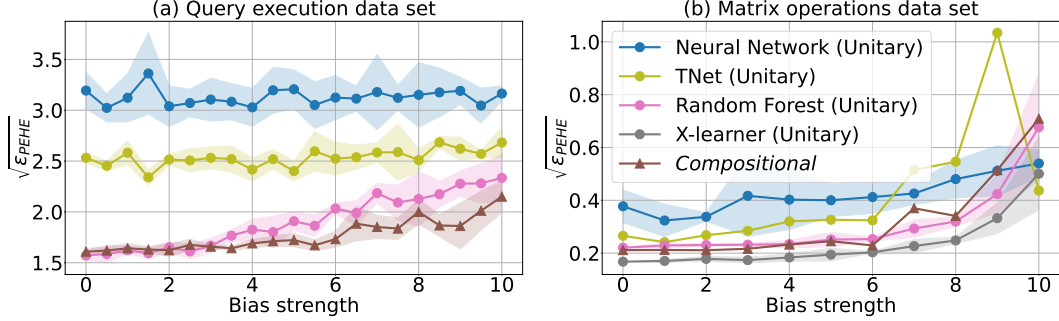


Figure 4: **Results for real-world data sets:** (a) *Query execution data set*: Compositional model estimates the effect more accurately as observational bias increases. (b) *Matrix operations data set*: All baselines perform similarly for this data set due to a single shared covariate, homogenous component outcome functions, and dominant contribution of matrix multiplication.

because covariate-based bias affects both unit-level and component-level balance, but the error of the compositional model is lower and increases more slowly than the unitary baselines.

When trained end-to-end, compositional models perform remarkably well even without component-level data access: Figure 3 reports the performance of models trained on synthetic data with varying degrees of data access. Figure 3(a) and (b) report results on a synthetic domain in which units have sequential and parallel structures, respectively. Compositional models outperform unitary models regardless of their access to component-level covariates and outcomes, demonstrating that compositional models can effectively estimate CATE for novel units in scenarios where component-level data is unavailable, and training uses only the compositional structure and unit-level data.

Unitary approaches compositionally generalize more easily for additive composition structures than sequential structures: The results in Figure 3 also show that unitary models can generalize for some composition types better than others. Figure 3(a) and (b) show results from units simulated with strictly sequential and (additive) parallel composition, respectively, with exactly the same component functions and covariate distributions. While most unitary models perform very poorly in the case of sequential composition, nearly all perform fairly well in the case of additive parallel composition, particularly as module combinations become more similar to the test data. The role of structure type in compositional generalization is often overlooked in relevant work in machine learning, where most work assumes either additive or sequential compositions.

Some factors can eliminate the advantages of compositional models for causal estimation: Figure 4(b) reports results for one realistic domain we studied — matrix operations — in which compositional models provide no substantial advantage over unitary baselines in both experimental (bias-strength = 0) and observational (bias-strength > 0) settings. This contrasts sharply with the superior performance of compositional models in the manufacturing (Figures 2, 3) and query execution (Figure 4(a)) domains. Further investigation identified three factors that explain this result: (1) the *dominance* of one component—matrix multiplication—in determining overall run-time (Figure 11); (2) *homogeneous* functional forms of the component outcome functions, such that additive composition leads to similar unit-level outcome functions (Figure 12); and (3) a *single shared covariate*—matrix size—that affects both unit-level and component-level outcomes, creating similar distribution imbalance issues at both the unit and component levels. In contrast, the query execution and manufacturing domains were more heterogeneous—different covariates affect component-level outcomes, no single component dominated in producing overall effects, component outcome functions belonged to different function classes, and composition structures were more complex. Thus, compositional models had higher relative performance in those domains.

6 Conclusion

The compositional models for causal effect estimation show promise in complex, modular, and heterogeneous systems. Compositional modeling provides a scalable and practical perspective

for instance-specific causal reasoning in modern technological systems. In this work, we focus on compositional models for shared treatment and individual effect estimation. Compositional causal reasoning about component-specific treatments, such as selecting the optimal configuration parameters for each component, and reasoning about the wide array of realistic interventions, such as adding, replacing, or removing components from the system, are useful directions for future work.

References

R. Ahsan, D. Arbour, and E. Zheleva. Learning relational causal models with cycles through relational acyclification. In *Proceedings of the AAAI Conference on Artificial Intelligence*, volume 37, pages 12164–12171, 2023.

J. Aldrich. Autonomy. *Oxford Economic Papers*, 41(1):15–34, 1989.

J. Andreas, M. Rohrbach, T. Darrell, and D. Klein. Neural module networks. In *Proceedings of the IEEE Conference on Computer Vision and Pattern Recognition*, pages 39–48, 2016.

S. Athey and G. Imbens. Recursive partitioning for heterogeneous causal effects. *Proceedings of the National Academy of Sciences*, 113(27):7353–7360, 2016.

D. Bahdanau, S. Murty, M. Noukhovitch, T. H. Nguyen, H. de Vries, and A. Courville. Systematic generalization: What is required and can it be learned? In *International Conference on Learning Representations*, 2019.

L. Bottou, J. Peters, J. Quiñonero-Candela, D. X. Charles, D. M. Chickering, E. Portugaly, D. Ray, P. Simard, and E. Snelson. Counterfactual reasoning and learning systems: The example of computational advertising. *Journal of Machine Learning Research*, 14(11), 2013.

W. Callebaut and D. Rasskin-Gutman. *Modularity: Understanding the Development and Evolution of Natural Complex Systems*. MIT press, 2005.

V. Chernozhukov, D. Chetverikov, M. Demirer, E. Duflo, C. Hansen, W. Newey, and J. Robins. Double/debiased machine learning for treatment and structural parameters. *The Econometrics Journal*, 21(1):C1–C68, 2018.

A. Curth and M. Van der Schaar. Nonparametric estimation of heterogeneous treatment effects: From theory to learning algorithms. In *International Conference on Artificial Intelligence and Statistics*, pages 1810–1818. PMLR, 2021.

A. Curth, R. W. Peck, E. McKinney, J. Weatherall, and M. van Der Schaar. Using machine learning to individualize treatment effect estimation: Challenges and opportunities. *Clinical Pharmacology & Therapeutics*, 2024.

A. D’Amour, P. Ding, A. Feller, L. Lei, and J. Sekhon. Overlap in observational studies with high-dimensional covariates. *Journal of Econometrics*, 221(2):644–654, 2021.

N. Friedman, L. Getoor, D. Koller, and A. Pfeffer. Learning probabilistic relational models. In *IJCAI*, volume 99, pages 1300–1309, 1999.

A. Gelman and J. Hill. *Data Analysis Using Regression and Multilevel/Hierarchical Models*. Cambridge University Press, 2006.

A. M. Gentzel, P. Pruthi, and D. Jensen. How and why to use experimental data to evaluate methods for observational causal inference. In *International Conference on Machine Learning*, pages 3660–3671. PMLR, 2021.

L. Getoor and B. Taskar. *Introduction to Statistical Relational Learning*. MIT press, 2007.

T. Haavelmo. The probability approach in econometrics. *Econometrica: Journal of the Econometric Society*, pages iii–115, 1944.

S. Harada and H. Kashima. Graphite: Estimating individual effects of graph-structured treatments. In *Proceedings of the 30th ACM International Conference on Information & Knowledge Management*, pages 659–668, 2021.

D. Heckerman and M. P. Wellman. Bayesian networks. *Communications of the ACM*, 38(3):27–31, 1995.

I. Higgins, N. Sonnerat, L. Matthey, A. Pal, C. Burgess, M. Bošnjak, M. Shanahan, M. Botvinick, D. Hassabis, and A. Lerchner. SCAN: Learning hierarchical compositional visual concepts. In *6th International Conference on Learning Representations, ICLR 2018-Conference Track Proceedings*, volume 6. International Conference on Learning Representations (ICLR), 2018.

J. L. Hill. Bayesian nonparametric modeling for causal inference. *Journal of Computational and Graphical Statistics*, 20(1):217–240, 2011.

P. W. Holland. Statistics and causal inference. *Journal of the American Statistical Association*, 81(396):945–960, 1986.

D. Hupkes, V. Dankers, M. Mul, and E. Bruni. Compositionality decomposed: How do neural networks generalise? *Journal of Artificial Intelligence Research*, 67:757–795, 2020.

R. A. Jacobs, M. I. Jordan, S. J. Nowlan, and G. E. Hinton. Adaptive mixtures of local experts. *Neural Computation*, 3(1):79–87, 1991.

D. Jarvis, R. Klein, B. Rosman, and A. M. Saxe. On the specialization of neural modules. In *The Eleventh International Conference on Learning Representations*, 2023.

C. T. Jerzak, F. D. Johansson, and A. Daoud. Image-based treatment effect heterogeneity. In *Conference on Causal Learning and Reasoning*, pages 531–552. PMLR, 2023.

F. Johansson, U. Shalit, and D. Sontag. Learning representations for counterfactual inference. In *International Conference on Machine Learning*, pages 3020–3029. PMLR, 2016.

F. D. Johansson, U. Shalit, N. Kallus, and D. Sontag. Generalization bounds and representation learning for estimation of potential outcomes and causal effects. *Journal of Machine Learning Research*, 23(166):1–50, 2022.

J. Kaddour, Y. Zhu, Q. Liu, M. J. Kusner, and R. Silva. Causal effect inference for structured treatments. *Advances in Neural Information Processing Systems*, 34:24841–24854, 2021.

E. H. Kennedy. Towards optimal doubly robust estimation of heterogeneous causal effects. *Electronic Journal of Statistics*, 17(2):3008–3049, 2023.

S. B. Khatami, H. Parikh, H. Chen, S. Roy, and B. Salimi. Graph neural network based double machine learning estimator of network causal effects. *arXiv preprint arXiv:2403.11332*, 2024.

E. Kochmar, D. D. Vu, R. Belfer, V. Gupta, I. V. Serban, and J. Pineau. Automated data-driven generation of personalized pedagogical interventions in intelligent tutoring systems. *International Journal of Artificial Intelligence in Education*, 32(2):323–349, 2022.

D. Koller and A. Pfeffer. Object-oriented Bayesian networks. In *Proceedings of the Thirteenth Conference on Uncertainty in Artificial Intelligence*, pages 302–313, 1997.

S. R. Künzel, J. S. Sekhon, P. J. Bickel, and B. Yu. Metalearners for estimating heterogeneous treatment effects using machine learning. *Proceedings of the National Academy of Sciences*, 116(10):4156–4165, 2019.

B. Lake and M. Baroni. Generalization without systematicity: On the compositional skills of sequence-to-sequence recurrent networks. In *International Conference on Machine Learning*, pages 2873–2882. PMLR, 2018.

B. M. Lake, R. Salakhutdinov, and J. B. Tenenbaum. Human-level concept learning through probabilistic program induction. *Science*, 350(6266):1332–1338, 2015.

K. B. Laskey. MEBN: A language for first-order Bayesian knowledge bases. *Artificial Intelligence*, 172(2-3):140–178, 2008.

S. Lee and V. Honavar. On learning causal models from relational data. In *Proceedings of the AAAI Conference on Artificial Intelligence*, volume 30, 2016.

S. Lippel and K. Stachenfeld. The impact of task structure, representational geometry, and learning mechanism on compositional generalization. In *ICLR 2024 Workshop on Representational Alignment*, 2024.

M. Maier, K. Marazopoulou, D. Arbour, and D. Jensen. A sound and complete algorithm for learning causal models from relational data. In *Proceedings of the Twenty-Ninth Conference on Uncertainty in Artificial Intelligence*, pages 371–380, 2013.

R. Marcus and O. Papaemmanouil. Plan-structured deep neural network models for query performance prediction. *Proceedings of the VLDB Endowment*, 12(11):1733–1746, 2019.

S. Mittal, Y. Bengio, and G. Lajoie. Is a modular architecture enough? *Advances in Neural Information Processing Systems*, 35:28747–28760, 2022.

J. Pearl. *Causality*. Cambridge University Press, 2009.

X. B. Peng, M. Chang, G. Zhang, P. Abbeel, and S. Levine. Mcp: Learning composable hierarchical control with multiplicative compositional policies. *Advances in Neural Information Processing Systems*, 32, 2019.

J. Peters, D. Janzing, and B. Schölkopf. *Elements of Causal Inference: Foundations and Learning Algorithms*. The MIT Press, 2017.

J. Pfeiffer, S. Ruder, I. Vulić, and E. M. Ponti. Modular deep learning. *arXiv preprint arXiv:2302.11529*, 2023.

P. R. Rosenbaum and D. B. Rubin. The central role of the propensity score in observational studies for causal effects. *Biometrika*, 70(1):41–55, 1983.

D. B. Rubin. Estimating causal effects of treatments in randomized and nonrandomized studies. *Journal of Educational Psychology*, 66(5):688, 1974.

D. B. Rubin. Causal inference using potential outcomes: Design, modeling, decisions. *Journal of the American Statistical Association*, 100(469):322–331, 2005.

B. Salimi, H. Parikh, M. Kayali, L. Getoor, S. Roy, and D. Suciu. Causal relational learning. In *Proceedings of the 2020 ACM SIGMOD International Conference on Management of Data*, pages 241–256, 2020.

S. Schug, S. Kobayashi, Y. Akram, M. Wolczyk, A. M. Proca, J. Von Oswald, R. Pascanu, J. Sacramento, and A. Steger. Discovering modular solutions that generalize compositionally. In *The Twelfth International Conference on Learning Representations*, 2024.

U. Shalit, F. D. Johansson, and D. Sontag. Estimating individual treatment effect: generalization bounds and algorithms. In *International Conference on Machine Learning*, pages 3076–3085. PMLR, 2017.

N. Shazeer, A. Mirhoseini, K. Maziarz, A. Davis, Q. Le, G. Hinton, and J. Dean. Outrageously large neural networks: The sparsely-gated mixture-of-experts layer. In *International Conference on Learning Representations*, 2016.

C. Shi, D. Sridhar, V. Misra, and D. Blei. On the assumptions of synthetic control methods. In *International Conference on Artificial Intelligence and Statistics*, pages 7163–7175. PMLR, 2022.

K. Shi, J. Hong, Y. Deng, P. Yin, M. Zaheer, and C. Sutton. Exedec: Execution decomposition for compositional generalization in neural program synthesis. In *The Twelfth International Conference on Learning Representations*, 2024. URL <https://openreview.net/forum?id=oTRwljRgiv>.

R. Socher, C. C. Lin, C. Manning, and A. Y. Ng. Parsing natural scenes and natural language with recursive neural networks. In *Proceedings of the 28th International Conference on Machine Learning (ICML-11)*, pages 129–136, 2011.

R. S. Sutton, D. Precup, and S. Singh. Between mdps and semi-mdps: A framework for temporal abstraction in reinforcement learning. *Artificial Intelligence*, 112(1-2):181–211, 1999.

B. Taskar, V. Chatalbashev, D. Koller, and C. Guestrin. Learning structured prediction models: A large margin approach. In *Proceedings of the 22nd International Conference on Machine Learning*, pages 896–903, 2005.

B. Van Niekerk, S. James, A. Earle, and B. Rosman. Composing value functions in reinforcement learning. In *International Conference on Machine Learning*, pages 6401–6409. PMLR, 2019.

S. Wager and S. Athey. Estimation and inference of heterogeneous treatment effects using random forests. *Journal of the American Statistical Association*, 113(523):1228–1242, 2018.

E. N. Weinstein and D. M. Blei. Hierarchical causal models. *arXiv preprint arXiv:2401.05330*, 2024.

T. Wiedemer, P. Mayilvahanan, M. Bethge, and W. Brendel. Compositional generalization from first principles. *Advances in Neural Information Processing Systems*, 36, 2024.

S. Witty and D. Jensen. Causal graphs vs. causal programs: The case of conditional branching. In *First Conference on Probabilistic Programming (ProbProg)*, 2018.

A Broader Impacts

This paper presents work that aims to advance the field of machine learning and causal inference. There are many potential societal consequences of our work, none of which must be specifically highlighted here.

B Other examples of structured systems with compositional data

The causal questions of interest in the compositional domain are: How do the unit-level interventions impact the component-level outcomes to produce the overall unit’s outcome? Many real-world phenomena require answering such causal questions about the effect of shared interventions on different components. We provide several real-world use cases where the compositional approach can be useful to reason about the effects of the interventions and make informed and personalized decisions.

- *Compiler optimization*: How do different hardware architectures (*intervention*) affect the compile time (*potential outcome*) of different source codes (*unit*)? In this case, source code consists of multiple program modules; hardware architecture is the unit-level intervention that can affect the compiling of different source codes differently, and compile time is the outcome of interest.
- *Energy efficiency optimization*: How does a state-wide mandate (*intervention*) of shifting to more efficient electric appliances affect the monthly bill (*potential outcome*) of each building (*unit*) in the state? Each building can be assumed to consist of various compositions of electric appliances. The intervention might affect the bill of each kind of appliance differently, affecting the overall utility bill.
- *Supply chain optimization*: How is the processing time (*potential outcome*) of an order (*unit*) affected when a supply chain company shifts to a different supplier for various parts (*intervention*)? In this case, each order execution plan is the unit of analysis that consists of routing the information from different parties, suppliers, manufacturers, and distributors specific to each order; intervention can impact the processing time of different parties depending on the affected parts and order details.
- *Causal reasoning in multi-agent systems*: How do the model hyperparameters (architecture, agent implementation types) affect the accuracy (potential outcomes) of multi-agent systems (LLM agents) for different task instances (*unit*)? As multi-agent LLM-based systems are becoming an integral part of daily workflows, developing instance-specific causal reasoning models for such systems using compositional approaches is helpful.

C Related Work

In this section, we discuss the connections of the compositional approach with the existing work in causal inference and associational machine learning in greater detail.

Causal effect estimation in structured domains: In causal inference, a relatively sparse body of work has focused on treatment effect estimation on structured data in modular domains [Gelman and Hill, 2006, Salimi et al., 2020, Kaddour et al., 2021]. For example, existing work in multi-level modeling and hierarchical causal models [Gelman and Hill, 2006, Witty and Jensen, 2018, Weinstein and Blei, 2024] leverages hierarchical data structure to improve effect estimation under unobserved confounders. There is also growing interest in heterogeneous effect estimation for complex data, such as images [Jerzak et al., 2023], structured treatments (e.g., graphs, images, text, drugs) [Harada and Kashima, 2021, Kaddour et al., 2021], and relational data [Salimi et al., 2020, Khatami et al., 2024]. The compositional approach complements this line of research by focusing on the units composed of multiple heterogeneous components. On the other hand, hierarchical causal models focus on units with hierarchical structures but homogeneous sub-units in a unit. Relational causal models primarily employ relational semantics to describe instance-specific structures and interactions among entities. The compositional approach uses simpler compositional semantics and focuses on the generic component-wise behavior of a system and interactions among them, where components can be objects, processes, and distinct heterogeneous modules in a system. Our focus also lies in

the structured and compositional representation of the units rather than only treatments, which helps better estimate causal effects in the case of high-dimensional observational data. Another piece of related work is the fine-grained analysis of the potential outcomes to study the validity of synthetic control methods with panel data [Shi et al., 2022]. This work focuses on reasoning about potential outcomes of homogeneous sub-units (individuals) to establish identifiability of unit-level (state) potential outcomes. The compositional approach employs similar fine-grained thinking and modeling, but exploits the availability of fine-grained data and proposes scalable approaches for modular causal reasoning.

Modularity and compositionality in SCMs: The vast body of work under the structural causal model (SCM) framework [Pearl, 2009] typically summarizes a system’s behavior with a fixed set of variables and assumes fixed causal structure among those variables (unless modified under explicit intervention via the do-operator). The causal model, a directed acyclic graph, represents the causal interactions among all variables. In the compositional approach, we assume an instance-specific structure among the components for a given unit. Thus, the compositional data-generating process could not be represented by a single SCM. Instead, a unique SCM corresponding to each unit structure would be required. This is beyond the scope of nearly all current work in SCMs, with a very few exceptions (e.g., [Laskey, 2008]).

In the specific context of structural causal models, the term *modularity* is sometimes used to refer to a model property in which the structural function of a given variable can be intervened upon without influencing the structural function of any other variable. This property is also known as *autonomy* [Haavelmo, 1944], *structural invariance* [Aldrich, 1989], and *independence of causal mechanism* [Peters et al., 2017]. Note that modularity, in this sense, is a property of the model—It is true by definition (variables in an SCM are assumed to be modular), and it is absolute. In contrast, the modular structure that we reference in this paper is a property of both the system being modeled and (perhaps) the structure of a given model of that system. In a compositional model, each component with specified inputs and outputs represents a module rather than a specific random variable, as usually assumed in SCMs. To enable compositional generalization, the compositional approach assumes that the data-generating distribution of outcomes of a component given component-specific inputs remains stable and invariant across the units *irrespective* of where the component appears in the structure of a unit. This assumption differs from the modularity assumption made in SCM, which assumes stability for the conditional distribution of each random variable given its parents in the direct graph.

Compositional models in associational machine learning: Our work is inspired by research on compositional models in machine learning that exploit the structure of underlying domains and explicitly represent it in the model structure [Heckerman and Wellman, 1995, Koller and Pfeffer, 1997, Friedman et al., 1999, Getoor and Taskar, 2007, Taskar et al., 2005, Laskey, 2008]. For example, research in object-oriented and relational models has produced directed graphical models that explicitly reproduce known modular structure in the systems being analyzed [Koller and Pfeffer, 1997, Friedman et al., 1999, Laskey, 2008]. In a similar way, modular architectures in deep neural networks have been designed to replicate the assumed modular structure of the systems that they attempt to model [Jacobs et al., 1991]. Some work in probabilistic programming has a similar flavor, in that the structure of the probabilistic program reflects known modular structure in the real-world system being analyzed [Lake et al., 2015]. The *instance-specific* modular architectures are widely used in machine learning to model data in natural language, program synthesis, reinforcement learning, and combined vision and language problems, providing sample efficiency, systematic generalization, and computation benefits [Andreas et al., 2016, Shazeer et al., 2016, Pfeiffer et al., 2023]. The closest work to the compositional models for causal effect estimation is using a mixture of expert (MoE) architecture [Jacobs et al., 1991, Shazeer et al., 2016] and modular neural networks [Socher et al., 2011, Andreas et al., 2016, Marcus and Papaemmanouil, 2019] in vision and language domains. However, most of the work in machine learning focuses on understanding the systematic generalization and sample efficiency benefits of compositional models for prediction tasks. At the same time, their role in reasoning about intervention effects is unexplored [Lake and Baroni, 2018, Hupkes et al., 2020, Mittal et al., 2022, Jarvis et al., 2023, Wiedemer et al., 2024, Schug et al., 2024, Lippel and Stachenfeld, 2024]. Additionally, compositionality is usually a property of the causal data-generating process, and viewing compositionality from the lens of causality, interventions, and components in the modular systems helps understand the compositional generalization characteristics of the models. This work takes the first step in that direction.

D Identifiability Results

D.1 Definition, assumptions and auxiliary lemmas

We first define the necessary distributions and provide some simple results. Assume that each unit i has pre-treatment covariates $\mathbf{X}_i = \mathbf{x} \in \mathcal{X} \subset \mathbb{R}^d$, a binary treatment $T_i \in \{0, 1\}$, and two potential outcomes $\{Y_i(0), Y_i(1)\} \in \mathcal{Y} \subset \mathbb{R}$ [Rubin, 1974, 2005]. In the observational data, we only observe one of the potential outcomes for each unit, $Y_i = Y_i(T_i)$ known as the *observed* or *factual* outcome and missing outcomes $Y_{iCF} = Y_i(1 - T_i)$ are known as *observed* or *counterfactual* outcome.

Definition D.1. *The conditional average treatment effect (CATE) is defined as*

$$\tau(x) : \mathbb{E}[Y_i(1) - Y_i(0) | \mathbf{X}_i = \mathbf{x}]$$

We first show that under the assumptions of ignorability and consistency, the CATE function $\tau(x)$ is identifiable by $\tau(\mathbf{x}) = \mathbb{E}[Y_i | \mathbf{X}_i = \mathbf{x}, T = 1] - \mathbb{E}[Y_i | \mathbf{X}_i = \mathbf{x}, T = 0]$ [Pearl, 2009] [Rosenbaum and Rubin, 1983]. We assume a joint distribution function $p(\mathbf{X}_i, T_i, Y_i(1), Y_i(0))$, such that $(Y_i(1), Y_i(0) \perp T_i) | \mathbf{X}_i$ and $0 < P(T = 1 | \mathbf{X}_i = \mathbf{x}) < 1$, for all \mathbf{x} . We also assume consistency; that is, we assume that we observe $y_i = Y_i(1) | T_i = 1$ and $y_i = Y_i(0) | T_i = 0$.

Lemma D.1.

$$\begin{aligned} & \mathbb{E}[Y_i(1) - Y_i(0) | \mathbf{X}_i = \mathbf{x}] \\ &= \mathbb{E}[Y_i(1) | \mathbf{X}_i = \mathbf{x}] - \mathbb{E}[Y_i(0) | \mathbf{X}_i = \mathbf{x}] \quad (2) \\ &= \mathbb{E}[Y_i(1) | \mathbf{X}_i = \mathbf{x}, T_i = 1] - \mathbb{E}[Y_i(0) | \mathbf{X}_i = \mathbf{x}, T_i = 0] \quad (3) \\ &= \mathbb{E}[Y_i | \mathbf{X}_i = \mathbf{x}, T_i = 1] - \mathbb{E}[Y_i | \mathbf{X}_i = \mathbf{x}, T_i = 0] \quad (4) \end{aligned}$$

Equality (2) is due to the linearity of the expectation. Equality (3) follows from the ignorability assumption in which we assume that $Y(T)$ is independent of T conditioned on \mathbf{X} . Equality (4) follows from the consistency assumption. The last equation consists of only observable quantities and can be estimated from the data if we assume overlap, $0 < P(T_i = 1 | \mathbf{X}_i = \mathbf{x}) < 1$, for all \mathbf{x} .

Definition D.2. *The conditional-average treatment effect (CATE) estimand for structured input $Q_i = q$ is defined as: $\tau(q) = \mathbb{E}[Y_i(1) - Y_i(0) | Q_i = q] = \mathbb{E}[Y_i(1) - Y_i(0) | Q_i = (G_i, \{\mathbf{x}_{ij}\}_{j=1:m_i})]$*

For ease of notation to describe conditional distributions, we denote the combined inputs to a component j as $\mathbf{Z}_j(t) = (\mathbf{X}_j, \{Y_l(t)\}_{l \in Pa(c_j)})$.

Definition D.3. *The conditional-average treatment effect (CATE) estimand for component j with $\mathbf{X}_j = \mathbf{x}_j \in \mathbb{R}^{d_j}$ is defined as: $\tau(\mathbf{z}_j) = \mathbb{E}[Y_i(1) - Y_i(0) | \mathbf{Z}_j = \mathbf{z}_j]$.*

D.2 Identifiability for hierarchical composition

We define the component-wise distributions as $P(Y(t) | \mathbf{Z}_j(t) = \mathbf{z}_j)$. In hierarchical composition, the unit outcome equals the final component outcome: $\mathbb{E}[Y_i(t) | Q_i = q] = \mathbb{E}[Y_{im_i}(t) | Q_i = q]$. This conditional expectation can be expressed by marginalizing intermediate component outcomes using the Markov assumption (Equation 1).

$$\mathbb{E}[Y_i(t) | Q_i = q] = \int_{Y_{im_i-1}(t)} \int_{Y_{im_i-2}(t)} \dots \int_{Y_{i1}(t)} \mathbb{E}[Y_{im_i}(t) | \mathbf{Z}_{im_i}(t)] \prod_{j=1}^{m_i-1} P(Y_{ij}(t) | \mathbf{Z}_{ij}(t)) \quad (5)$$

We use the following nested expectation expression as shorthand for marginalization over intermediate component outcomes:

$$\mathbb{E}[Y_i(t) | Q_i = q] = \mathbb{E}_{Y_{i1:im_i-1}(t)} [\mathbb{E}[Y_{im_i}(t) | \mathbf{Z}_{im_i}(t)]] \quad (6)$$

Assumption E (Component-level ignorability). *The component level potential outcomes and assigned treatment are independent conditioned on the component level covariates, i.e., $Y_j(1), Y_j(0) \perp T | \mathbf{X}_j$.*

Assumption F (Component-level overlap). *The overlap holds for the component level covariates $X_j = x_j$, i.e., $\forall x_j \in \mathcal{X}_j, t \in \{0, 1\} : 0 < p(T = t | \mathbf{X}_j = \mathbf{x}_j) < 1$*

Assumption G (Component-level consistency). *The consistency holds for the component level covariates, i.e., $y_j = Y_j(0)|t = 0$ and $y_j = Y_j(1)|t = 1$.*

As the treatment is assigned before any component's potential outcomes are observed, we can assume that the component's covariates \mathbf{X}_j are sufficient to satisfy ignorability assumptions, i.e., $Y_j(t) \perp T|X_j$. Consider the conditional distribution $P(Y_j(t)|\mathbf{Z}_j(t))$. Assuming component-level ignorability for component j , we can write

$$\begin{aligned} P(Y_{ij}(t)|\mathbf{Z}_{ij}(t)) &= P(Y_{ij}(t)|\mathbf{X}_j, \{Y_l(t)\}_{l \in Pa(c_j)}) \\ &= P(Y_{ij}|\mathbf{X}_j, \{Y_l(t)\}_{l \in Pa(c_j)}, T = t) \end{aligned}$$

Now, assuming consistency for components c_l , where $l \in Pa(c_j)$, we can write $Y_l(t)|T = t = Y_l$.

$$P(Y_{ij}(t)|\mathbf{Z}_{ij}(t)) = P(Y_{ij}|\mathbf{X}_j, \{Y_l\}_{l \in Pa(c_j)}, T = t) = P(Y_{ij}|\mathbf{Z}_{ij}, T = t)$$

Similarly, $\mathbb{E}[Y_{im_i}(t)|\mathbf{Z}_{im_i}(t)]$ can be written as $\mathbb{E}[Y_{im_i}|\mathbf{Z}_{im_i}, T = t]$, assuming component-level ignorability and consistency. Substituting these quantities in Equation 5, we get the below result.

$$\begin{aligned} \tau(q) &= \int_{Y_{im_i-1}} \int_{Y_{im_i-2}} \dots \int_{Y_{i1}} \mathbb{E}[Y_{im_i}|\mathbf{Z}_{im_i} = \mathbf{z}_{im_i}, T = 1] \prod_{j=1}^{im_i-1} P(Y_{ij}|\mathbf{Z}_{ij} = \mathbf{z}_{iz}, T = 1) - \\ &\quad \int_{Y_{im_i-1}} \int_{Y_{im_i-2}} \dots \int_{Y_{i1}} \mathbb{E}[Y_{im_i}|\mathbf{Z}_{im_i} = \mathbf{z}_{im_i}, T = 0] \prod_{j=1}^{im_i-1} P(Y_{ij}|\mathbf{Z}_{ij} = \mathbf{z}_{iz}, T = 0) \end{aligned}$$

Using shorthand notation, we get the desired result.

$$\tau(q) = \mathbb{E}_{Y_{1:m_i-1}} [\mathbb{E}[Y_{m_i}|\mathbf{Z}_{m_i} = \mathbf{z}_{m_i}, T = 1]] - \mathbb{E}_{Y_{1:m_i-1}} [\mathbb{E}[Y_{m_i}|\mathbf{Z}_{m_i} = \mathbf{z}_{m_i}, T = 0]]$$

Component-level overlap assumption ensures that the estimand is identified using observational data.

G.1 Identifiability for additive parallel composition

In this section, we first describe the assumptions that the data-generating process follows for additive parallel composition. Then, we prove the identifiability results for additive parallel composition.

Assumption H. *Additivity assumes that the ground-truth component-level potential outcomes add up to generate the ground-truth unit-level potential outcome, i.e., $Y_i(1) = \sum_{j=1}^{m_i} Y_{ij}(1)$, $Y_i(0) = \sum_{j=1}^{m_i} Y_{ij}(0)$.*

Assumption I. *Conditional independence assumption among potential outcomes implies that the ground-truth potential outcomes of a component j are conditionally independent of outcomes of other components l ($l \neq j$) given the component's covariates \mathbf{X}_j : $Y_j(T) \perp Y_l(T)|\mathbf{X}_j$*

Assuming conditional independence assumption and Markov assumption, the data-generating process for additive parallel composition can be written as: $Y_{ij}(t) = \mu_{ot}(\mathbf{X}_{ij}) + \epsilon_{io}(t)$

Assuming additivity assumption H, we get

$$\tau(q) = \mathbb{E}[\sum_{j=1}^{m_i} Y_{ij}(1) - \sum_{j=1}^{m_i} Y_{ij}(0)|Q_i = (G_i, \{\mathbf{x}_{ij}\}_{j=1:m_i})]$$

Due to the linearity of the expectation, we get the following:

$$\tau(q) = \mathbb{E}[\sum_j^{m_i} Y_{ij}(1)|Q_i = (G_i, \{\mathbf{x}_{ij}\}_{j=1:m_i})] - \mathbb{E}[\sum_j^{m_i} Y_{ij}(0)|Q_i = (G_i, \{\mathbf{x}_{ij}\}_{j=1:m_i})]$$

Assuming conditional independence assumption among the component-level potential outcomes and Markov assumption, we get

$$\tau(q) = \sum_{j=1}^{m_i} \mathbb{E}[Y_{ij}(1)|\mathbf{x}_{ij}] - \mathbb{E}[Y_{ij}(0)|\mathbf{x}_{ij}] = \sum_{j=1}^{m_i} \mathbb{E}[Y_{ij}(1) - Y_{ij}(0)|\mathbf{x}_{ij}] = \sum_{j=1}^{m_i} \tau(\mathbf{x}_{ij})$$

Now, we prove the identifiability result for additive parallel composition.

$$\tau(q) = \sum_{j=1}^{m_i} \mathbb{E}[Y_{ij}(1)|\mathbf{x}_{ij}] - \mathbb{E}[Y_{ij}(0)|\mathbf{x}_{ij}]$$

Assuming component-level ignorability, we get

$$\tau(q) = \sum_{j=1}^{m_i} \mathbb{E}[Y_{ij}(1)|\mathbf{x}_{ij}, T=1] - \mathbb{E}[Y_{ij}(0)|\mathbf{x}_{ij}, T=0]$$

Assuming component-level consistency, we get

$$\tau(q) = \sum_j^{m_i} \mathbb{E}[Y_{ij}|\mathbf{x}_{ij}, T=1] - \mathbb{E}[Y_{ij}|\mathbf{x}_{ij}, T=0]$$

Component-level overlap assumption ensures the estimand is identified using observational data.

J Learning compositional models from observational data

In this section, we first discuss the modified algorithm for the hierarchical composition model to facilitate the modeling of noise variables ϵ_{ot} (assuming zero-mean additive noise variables in Equation 1) along with the *expected* potential outcome functions μ_{ot} . This allows the marginalization of intermediate component-level potential outcomes to obtain unit-level CATE estimates for sequential and hierarchical compositions. Then, we discuss the additive parallel composition model case.

J.1 Hierarchical composition model (modeling the distribution $P(Y_j(t)|\mathbf{Z}_j(t))$)

Model Training: The component models for estimating mean and variance of conditional distribution of the component-level potential outcomes are denoted by $(\hat{f}_{\theta_o}, \hat{\sigma}_{\psi_o}^2) : \mathbb{R}^{d_o} \times \mathbb{R}^D \times \{0, 1\} \rightarrow \mathbb{R} \times \mathbb{R}^+$, assuming maximum in-degree of the graph G_i as D . Each model corresponding to component class $o \in \{1, 2, \dots, k\}$ is parameterized by separate and independent parameters θ_o for the mean and ψ_o for the variance. For a given observational data set with n samples, $\mathcal{D}_F = \{q_i, t_i, y_i\}_{i=1:n}$, we assume that we observe component-level features $\{\mathbf{x}_{ij}\}_{j=1:m_i}$, assigned treatment t_i and fine-grained component-level potential outcomes $\{y_{ij}\}_{j=1:m_i}$ along with unit-level potential outcomes y_i . If component instance $c_j \in M_o$, training of each component model o involves the independent learning of the parameters by minimizing the *negative log-likelihood loss*: $(\theta_o^*, \psi_o^*) := \arg \min \theta_o, \psi_o \frac{1}{N_o} \sum_{m=1}^{N_o} \left[\frac{1}{2} \log(2\pi \hat{\sigma}_{\psi_o}^2(\mathbf{z}_m, t_m)) + \frac{(y_{ij} - \hat{f}_{\theta_o}(\mathbf{z}_m, t_m))^2}{2\hat{\sigma}_{\psi_o}^2(\mathbf{z}_m, t_m)} \right]$ where N_o denotes the total number of component instances of component class o across all the N samples, and m denotes the index of the component instance in class o .

Model Inference: To estimate the CATE for a unit i , a modular architecture consisting of m_i component models is instantiated with the same input and output structure as G_i . During inference for treatment $T = t$, the predictions of potential outcomes of the parent's components $\{\hat{y}_{lt}\}_{l \in Pa(c_j)}$, $l \in M_o$ are sampled from a normal distribution $\hat{y}_{lt} \sim N(\hat{\mu}_{ot}, \hat{\sigma}_{ot}^2)$. We slightly abuse the notation to denote the inferred variance and variance model using σ^2 .

The mean and variance of the j^{th} component outcome are obtained using these samples.

$$\begin{aligned} \hat{\mu}_{jt} &= \hat{f}_{\theta_o^*}(\mathbf{x}_j, \{\hat{y}_{lt}\}_{l \in Pa(c_j)}, t) = \hat{f}_{\theta_o^*}(\hat{z}_{jt}, t) \\ \hat{\sigma}_{jt}^2 &= \hat{\sigma}_{\psi_o^*}^2(\mathbf{x}_j, \{\hat{y}_{lt}\}_{l \in Pa(c_j)}, t) = \hat{\sigma}_{\psi_o^*}^2(\hat{z}_{jt}, t) \end{aligned}$$

The estimate $\mathbb{E}[Y_i(1) - Y_i(0)|Q_i = q]$ of CATE is obtained through Monte Carlo integration by averaging over S samples: $\hat{\tau}(q) \approx \frac{1}{S} \sum_{s=1}^S [\hat{f}_{\theta_o^*}(\hat{z}_{m_i t}^{(s)}, 1) - \hat{f}_{\theta_o^*}(\hat{z}_{m_i t}^{(s)}, 0)]$, where each sample path $\hat{z}_{m_i t}^{(s)}$ is generated by hierarchically sampling from the component distributions: $\hat{y}_{jt}^{(s)} \sim \mathcal{N}(\hat{\mu}_{jt}, \hat{\sigma}_{jt}^2)$ for $j = 1$ to $m_i - 1$.

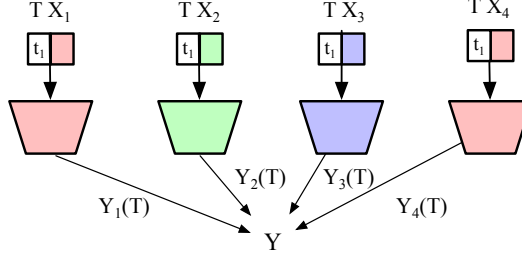


Figure 5: Model architecture for parallel composition model

J.2 Additive Parallel Composition Model

The key idea is that the component-level models for effect estimation are instantiated specific to each unit, and outcomes of one component are not shared with other components as we assume conditional independence among the potential outcomes given component-level features and shared treatment. In addition, linearity of expectation applies to the additive composition model, so we can directly compute the CATE estimates by just estimating the expected component-level potential outcomes. See Figure 5 for model architecture for parallel composition.

Model Training: The component models for estimating component-level potential outcomes are denoted by $\hat{f}_{\theta_o} : \mathbb{R}^{d_o} \times \{0, 1\} \rightarrow \mathbb{R}$. Each model corresponding to component class $o \in \{1, 2, \dots, k\}$ is parameterized by separate and independent parameters θ_o . For a given observational data set with n samples, $\mathcal{D}_F = \{q_i, t_i, y_i\}_{i=1:n}$, we assume that we observe component-level features $\{\mathbf{x}_{ij}\}_{j=1:m_i}$, assigned treatment t_i and fine-grained component-level potential outcomes $\{y_{ij}\}_{j=1:m_i}$ along with unit-level potential outcomes y_i . If component instance $c_j \in M_o$, training of each component model o involves the independent learning of the parameters by minimizing empirical risk: $\theta_o^* := \arg \min_{\theta_o} \frac{1}{N_o} \sum_{m=1}^{N_o} (\hat{f}_{\theta_o}(\mathbf{x}_m, t_m) - y_m)^2$, where N_o denotes the total number of component instances of component class o across all the N samples, and m denotes the index of the component instance belonging to class o . To clarify, t_m denotes the assigned treatment T_i for the unit i from which component instance m data sample is obtained, and y_m is the corresponding component-level outcome. The potential outcome of each component is computed using input features of that component, shared unit-level treatment, and *observed* potential outcomes of the parent's component.

Model Inference: To estimate CATE for a unit i , a modular architecture consisting of m_i component models is instantiated with the same number of components as in the unit i . During inference for treatment $T = t$, due to conditional independence assumption, $\hat{y}_{ijt} = \hat{f}_{\theta_o^*}(\mathbf{x}_{ij}, t)$. The estimate of CATE is obtained by taking the sum of the potential outcome estimates of all component instances $\hat{\tau}(q) = \sum_{j=1, j \in M_o}^{m_i} \hat{f}_{\theta_o^*}(\mathbf{x}_{ij}, 1) - \hat{f}_{\theta_o^*}(\mathbf{x}_{ij}, 0)$.

J.3 Relaxing assumptions about component-level data access for additive parallel composition

The model description above assumes observed component-level covariates and outcomes. This assumption is often reasonable, given the wide availability of fine-grained data for many structured domains. However, other cases exist when only the unit-level covariates \mathbf{X} and outcomes \mathbf{Y} are observed, and the component-level covariates \mathbf{X}_j and outcomes \mathbf{Y}_j are unobserved. Below, we discuss hierarchical composition models for these cases.

Case 1: Unobserved \mathbf{X}_j , observed \mathbf{Y}_j : We jointly learn the lower-dimensional component-level representations $\phi_o : \mathbb{R}^d \times \mathbb{R}^{d'_o}$, as well as the parameters of outcome functions. If we assume component instance $c_j \in M_o$, then $\hat{f}_{\theta_o} : \theta_o := \arg \min_{\theta} \frac{1}{N_o} \sum_{i=1}^{N_o} (\hat{f}_{\theta_o}(\phi_o(\mathbf{x}_i), t_i) - y_{ij})^2$. ϕ_o is jointly trained with the parameters θ_o , so that the relevant variables for predicting y_{ij} are selected.

Case 2: Observed \mathbf{X}_j , unobserved \mathbf{Y}_j : The model architecture remains the same as before, but we do not have individual component-level loss functions and only know the loss function for unit-level outcomes. Due to this, the parameters of the components are jointly learned to optimize the loss of estimating unit-level outcomes. Due to additive composition, the joint loss function is given by: $[\theta_1, \theta_2, \dots, \theta_k] := \arg \min_{\Theta} \frac{1}{N} \sum_{i=1}^N (\hat{f}_{\theta_{m_i}} + \hat{f}_{\theta_{m_{i-1}}} + \dots + \hat{f}_{\theta_1}(\mathbf{x}_{i1}, t) - y_i)^2$

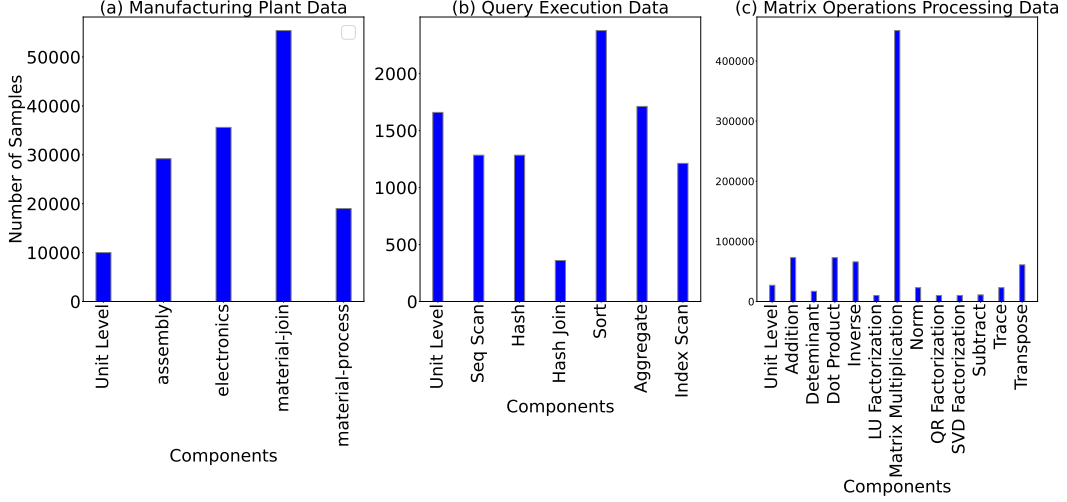


Figure 6: **Number of samples for units and component instances for different domains:** (a) Manufacturing data set showing component re-use across layouts (10,000 units). (b) Query execution data set (1,500 units). (c) Matrix operations processing data set (25,000 units)

Case 3: *Unobserved X_j and *unobserved Y_j* :* In this case, we only assume the knowledge of G_i . In this case, the model is equivalent to a mixture of experts (MoE) [Jacobs et al., 1991] architecture with addition as gating function. $[\theta_1, \theta_2 \dots \theta_k] := \arg \min_{\Theta} \frac{1}{N} \sum_{i=1}^N (\hat{f}_{\theta_{m_i}} + \hat{f}_{\theta_{m_{i-1}}} + \dots + \hat{f}_{\theta_1}(\phi_1(\mathbf{x}_i), t) - y_i)^2$

K Experimental Infrastructure

K.1 Data sets

In this section, we describe the details of the two benchmarks based on real-world computational systems — query execution, matrix operations and one benchmark based on a realistic simulation — manufacturing plant data.

K.1.1 Query Execution System

We first collect 10000 most popular user-defined Math Stack Overflow queries. We install a PostgreSQL 14 database server and load a 50 GB version of the publicly available Stack Overflow Database. We then run these queries with different combinations of the configuration parameters listed in Table 1. In all our experiments, our queries were executed with PostgreSQL 14 database on a single node with an Intel 2.3 GHz 8-Core Intel Core i9 processor, 32GB of RAM, and a solid-state drive. PostgreSQL was configured to use a maximum of 0 parallel workers to ensure non-parallelized executions so that additive assumption about operations is satisfied (`max_parallel_workers_per_gather = 0`). Before each run of the query, we begin from the cold cache by restarting the server to reduce caching effects among queries. Many database management systems provide information about the query plans as well as actual execution information through convenient APIs, such as EXPLAIN ANALYZE queries. Usually, Postgres reports the total run-time of each operation, along with children’s operations. We mainly model the query plans with the following operations — Sequential Scan, Index Scan, Sort, Aggregate, Hash, Hash Join as the occurrence of these operations in collected query plans was good, providing a large number of samples to learn the models from data. For CATE estimation experiments, we select 1500 query plans in which effect sizes were significant and were actually a result of the intervention rather than random variation in the run-time due to the stochastic nature of the database execution system. Each SQL query is run 5 times, and the median execution time is taken as the outcome. We evaluate the combined treatment effect of increasing working memory size and adding indices on structured query execution plans (Table 1). Increasing working memory affects the run-time of sorting, hash join, and aggregation operations, as can be seen in Figure 7. Adding

additional indices modifies the structure of the execution plan by switching from a sequential scan component to an index scan component, as discussed below.

Treatment	Working Memory	Temp Buffers	Indices
T=0	64 KB	800 KB	Primary key indexing
T=1	50 MB	100 MB	Secondary key indexing

Table 1: Treatment details for query execution data set

Change in the structure of query execution plans as a result of interventions on configuration parameters:

For some interventions on the configuration parameters and for some queries, the query planner doesn't return the same query plan. It returns the query plan with a changed structure as well as modified features of the components. This makes sense as that is the goal of query optimizers to compare different plans as resources change and find the most efficient plan. For example, increasing the working memory often causes query planners to change the ordering of Sort and aggregate operations, changing the structure as well as inputs to each component. These interventions are different from standard interventions in causal inference in which we assume that the covariates of the unit remain the same (as they are assumed to be pre-treatment) and treatment only modifies the outcome. In this case, a few features of the query plan are modified as a result of the intervention (and thus are post-treatment), while other features remain the same. Prediction of which features would change is part of learning the behavior of the query planner under interventions. In this work, we have mostly focused on learning the behavior of the query execution engine and assumed that the query planner is accessible to us. For simplicity, we assume that we know of the change in structure as a result of the intervention for both models. We leave the learning of the behavior of query optimizers under interventions for future work. This case provides another challenge for the task of causal effect estimation, even in the case of randomized treatments (bias strength = 0); due to the modified features of the query plans, the distribution of features in control and treatment populations might differ, providing an inherent observational bias in the dataset coming from the query optimizer. As long as we provide the information about modified query plans for both models, we believe that our comparisons are fair. For changed query structure, CATE estimand can be thought of as conditional on the same query but two different query plans.

$$\begin{aligned}\tau(Q_i) &= \mathbb{E}[Y_i(1) - Y_i(0)|Q_i] \\ \tau(Q_i) &= \mathbb{E}[\mathbb{E}[Y_i(1)|Q_{p_i}(1)] - \mathbb{E}[Y_i(0)|Q_{p_i}(0)]]\end{aligned}$$

Covariates used for query execution data for model training: See Table 2 for information about the high-dimensional covariates and component-specific covariates used for training models on query execution plans data set.

K.1.2 Manufacturing Plant Data

We use a process-based discrete-event simulation framework, Simpy, to generate realistic manufacturing plant data. The plant aims to produce the final product by processing raw materials and assembling intermediate parts. The simulation comprises **four** distinct manufacturing processes: Material Processing, Material Joining, Electronics Processing, and Assembly combined and re-used across 50 manufacturing line layouts with varying hierarchical structures. Each scenario consists of simulations with product demand varying from 5 to 1000, with different raw material inventories (pre-treatment covariates) available for each demand. The intervention consists of the availability of multiple workers with two different skill levels – (1) 5 workers with a higher mean of skill distribution and (2) 15 workers with a lower mean of skill distribution (Figure 9). The goal is to estimate the effect of workers' (with different skill levels) availability on the number of parts produced. Figure 10 shows the effect of treatment on total output (total number of parts produced), total time (total processing time of each scenario), and output per time (total parts produced/time) distributions. This data satisfies causal Markov dependence among the potential outcomes as the quality of the part processed by the component is explained by the raw-material inputs, intervention, and the quality of the directly connected parent components. There are a total of 39 unit-level covariates and around 10 covariates per component.

A factory has the following features:

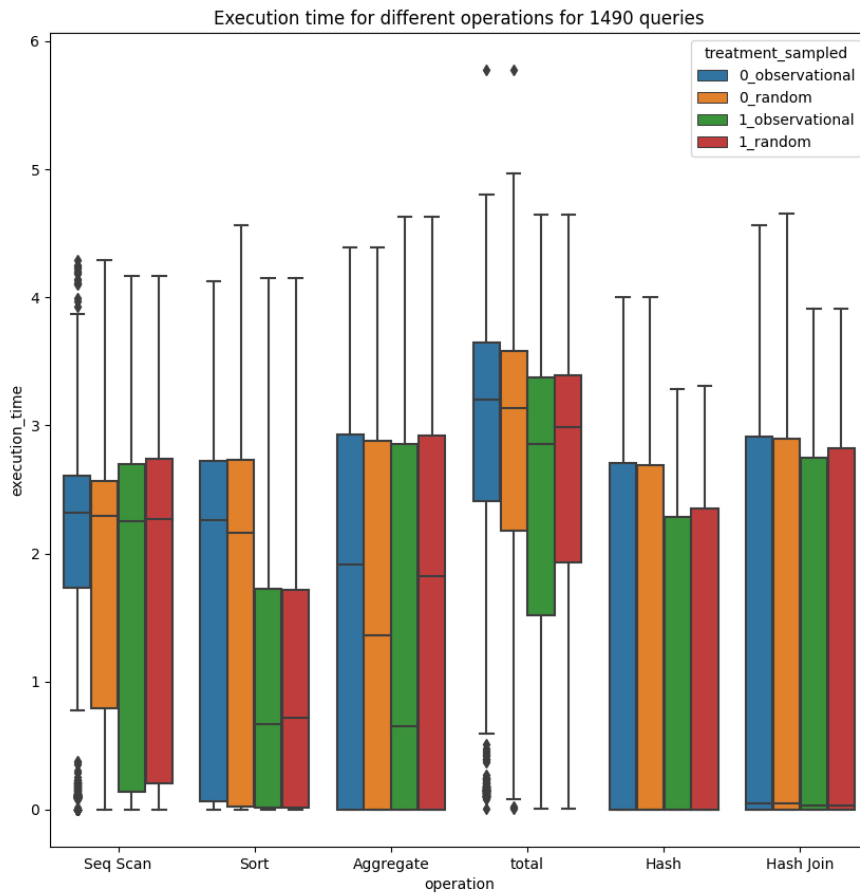


Figure 7: **Treatment effect on query executions for 1500 queries:** Ground-truth causal effect estimate of increasing memory for experimental data (random) and observational data created with bias strength = 1. 0 means low memory, and 1 means high memory. We can see that increasing memory has the most effect on sort and aggregate operation and the least effect on the sequential scan.

Model	Component	Training features	Outcome
Unitary		num_Sort, num_Hash_Join, num_Seq_Scan, num_Hash, num_Index_Scan, num_Aggregate, num_complex_ops, Sort_input_rows, Hash Join_input_rows, Hash Join_left_plan_rows, Hash Join_right_plan_rows, Seq Scan_input_rows, Hash_input_rows, Index Scan_input_rows, Aggregate_input_rows	total_time
Compositional	Sequential Scan	Seq_Scan_input_rows, Seq_Scan_plan_rows	seq_scan_time
Compositional	Index Scan	Index_Scan_input_rows, Index_Scan_plan_rows	index_scan_time
Compositional	Hash	Hash_input_rows, Hash_plan_rows	hash_time
Compositional	Hash Join	Hash_Join_left_input_rows, Hash_Join_right_input_rows, Hash_Join_plan_rows	hash_join_time
Compositional	Sort	Sort_input_rows, Sort_plan_rows	sort_time
Compositional	Aggregate	Aggregate_input_rows, Aggregate_plan_rows	aggregate_time

Table 2: Covariates used by unitary and compositional models for query execution plans data set

1. **Inventory of raw items** (Covariates): This includes parts and items which come into the factory to be processed into a final product. For this example, we use the following:
 - (a) *Fastener*: This includes parts such as screws, nuts and bolts.
 - (b) *Electronic component*: electronic components are parts used in the assembly of electronic assemblies such as printed circuit boards.
 - (c) *Raw material*: These are parts such as metal blanks, plastic sheets, sheet-metal etc.
 - (d) *Misc Component*: Parts such as belts, pulleys, gears etc.
2. **Process archetypes** (Components): These are processing stations which consume inventory of raw items and parts from other processes to produce a part. A process is defined by its processing time, i.e. how long does it ideally take to produce the part, and complexity, i.e how complex the given task is. Archetypes used in this simulation are:
 - (a) *Material Processing*: takes 1 part, does some processing and outputs the processed part (eg: painting, coating, heat treatment etc.)
 - (b) *Material Joining*: takes two parts and joins them together to output another part (eg: welding, riveting, fasteners to put two parts together)
 - (c) *Electronics Processing*: takes multiple components and electronics to produce a electronic part (eg: soldering, PCB manufacturing)
 - (d) *Assembly*: takes components from other stations and puts them together to form an assembly (eg: final product assembly)
3. **Workers** (Treatment): workers are a common resource pool of people working on a process. At a given time one process can have only one worker. A worker is defined by their skill which directly impacts how long a process will take over its base time and how much scrap (the final part is unusable and cannot proceed to the next step) and rework (redo aspects of the process increasing the amount of time the process takes) the process may produce.

K.1.3 Matrix operations processing

We generate a matrix operations data set by evaluating complex 25 complex matrix expressions on two computer hardware with different processors and RAM (treatment) and evaluate the execution time for each treatment (potential outcomes). The matrix size of matrices varies from 2 to 1000, resulting in total 25000 unit samples. The expressions contain 12 component operations, e.g., matrix

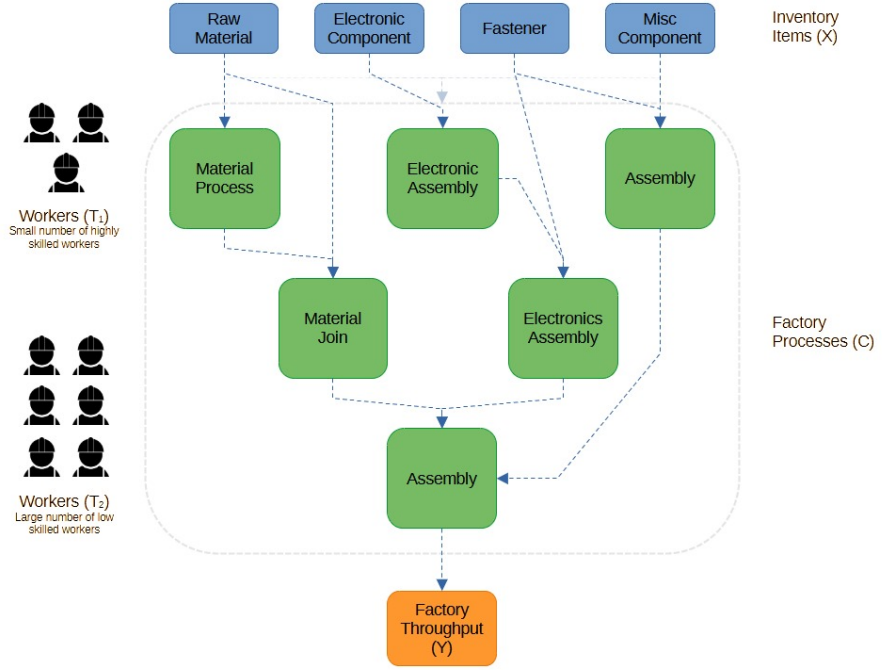


Figure 8: Illustrative figure explaining manufacturing assembly system

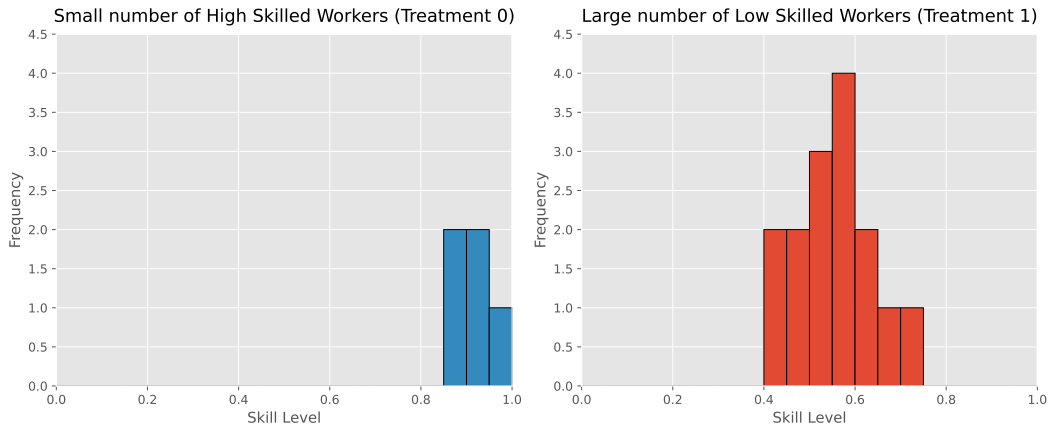


Figure 9: **Treatment for manufacturing plant data:** skill distribution for five (5) vs. fifteen (15) skilled workers.

multiplication, inverse, singular value decomposition, etc. We ensure each operation is executed individually, ensuring parallel composition with additive aggregation function. Matrix size is used as a biasing covariate to create a distribution mismatch between treatment groups. Treatment 0 means operations are processed on computer hardware with an 8-core, 32GB of RAM, and treatment 1 means operations are processed on 1-core, 4 GB RAM. Figure 12 shows the potential outcome functions for each treatment for unit-level and component data. Figure 11 shows that the matrix multiplication operation is the dominant operation, taking the most of the execution time (50%) across all matrix expressions

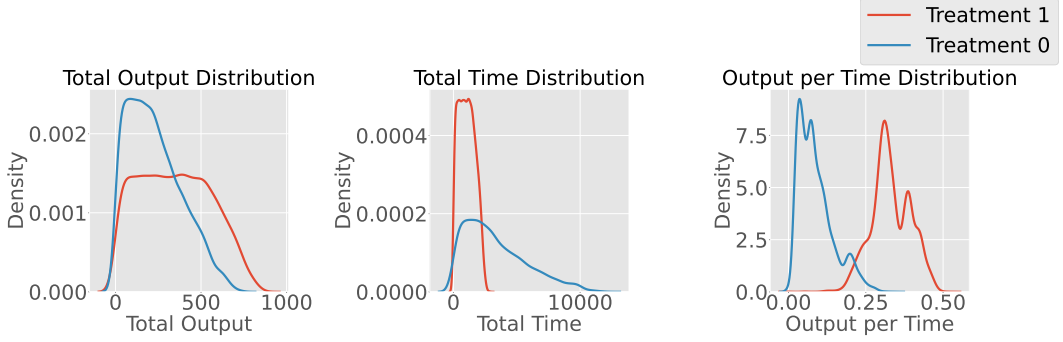


Figure 10: **Distribution of different potential outcomes for manufacturing data** : This figure shows the distribution of various potential outcomes for treatment and control groups for manufacturing plant data — (a) total output (total number of parts produced), (b) total time (total processing time of each scenario), and (c) output per time (total parts produced/time) distributions. We consider total output (total number of parts produced (a)) in our experiments.

Mean Percentage Time of component operation as compared to the total time

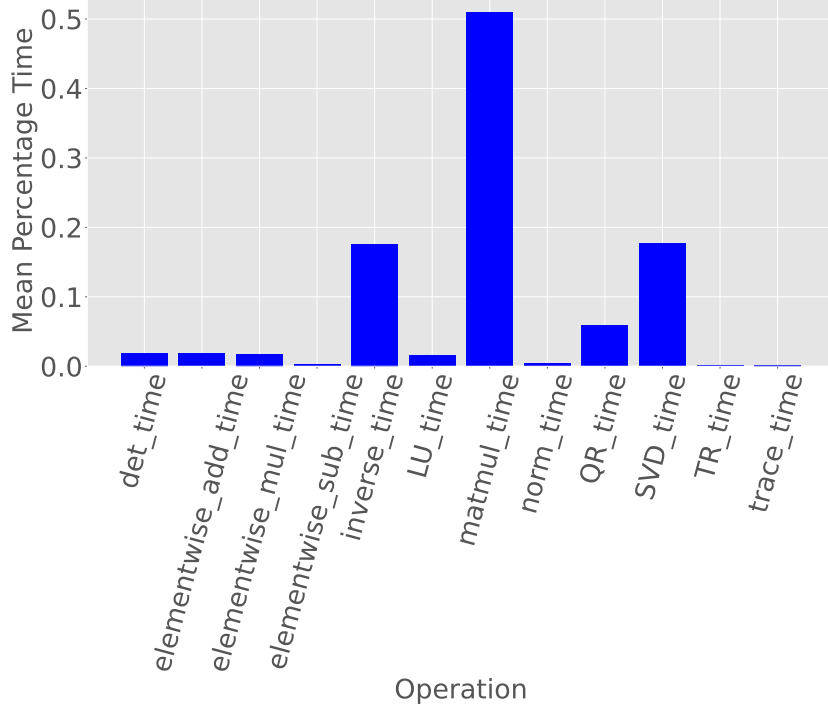


Figure 11: **Dominant contribution of component operation in total execution time**: This figure shows the dominant contribution of matrix multiplication’s execution time in total execution time. Percentage contribution of each component is calculated for each unit. Mean is taken over 25000 unit instances corresponding to 25 expression structures.

K.1.4 Synthetic data generation:

We generate data sets with varying characteristics to test model performance for units with different structures and composition functions. Structured units are generated by sampling binary trees (max depth=10) with $k=10$ heterogeneous modules, each having $d_j=1$ feature ($d=10$ (covariates) + 10 (structural information) total). All components’ total sum of features is used as a biasing covariate to create a distribution mismatch based on joint covariates distribution. For observational bias based on the structure, the depth of the trees is used as a proxy for structural information. The covariate distribution for each component is sampled from a multivariate Gaussian and uniform distribution

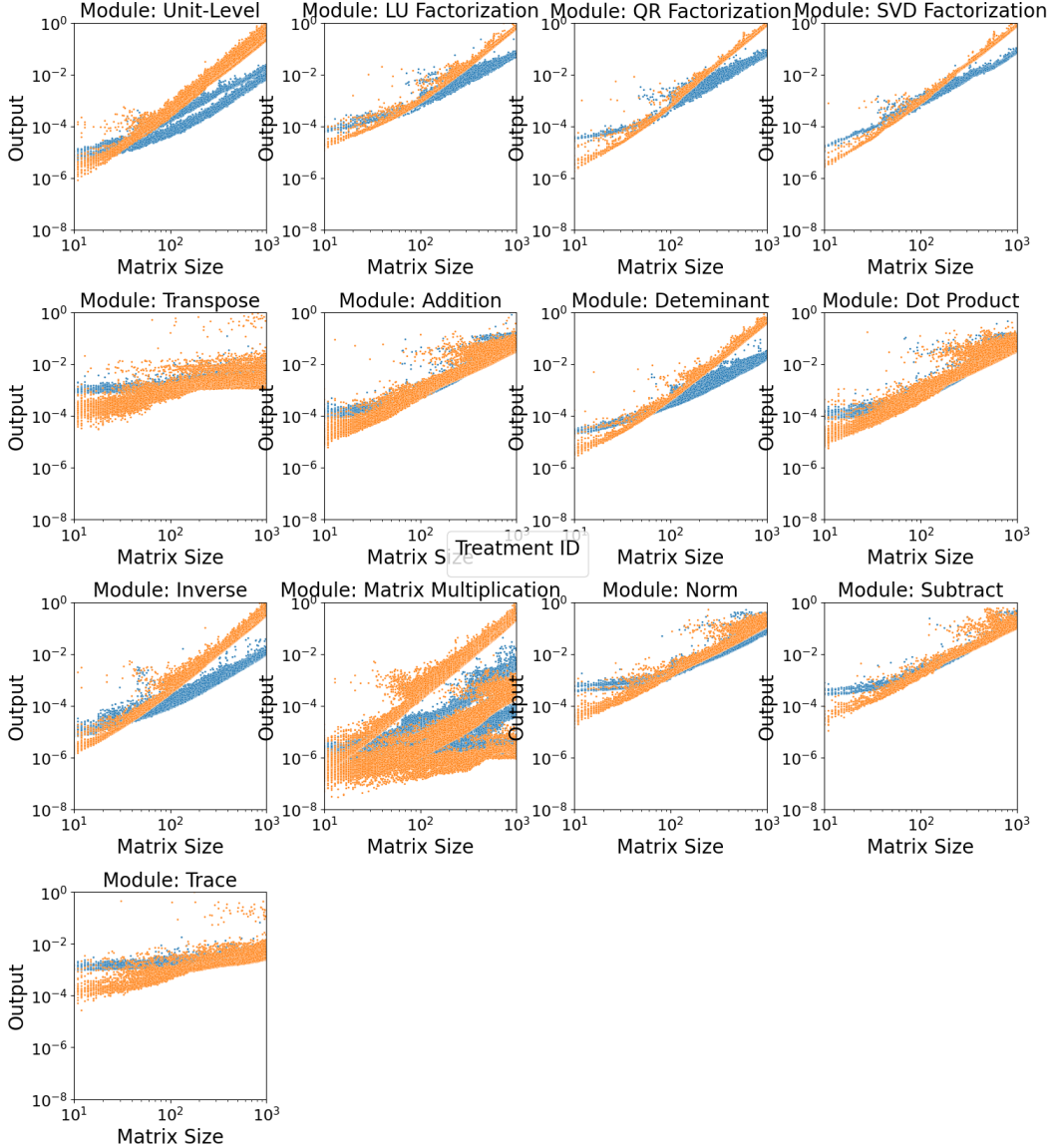


Figure 12: **Homogeneous functional forms of the component outcome function for matrix operations data set:** Ground-truth outcome functions for components for matrix operation data set. Blue and orange colors correspond to binary treatments 0 and 1. Intervention corresponds to two different compute hardware on which matrix expressions are processed.

with a mean ranging between 0 and 3 and covariance ranging between 0 and 3. The potential outcome for each treatment is a polynomial smooth function with different parameters for each treatment to generate heterogeneous treatment effects. For fixed structure data generation, the depth of the tree is fixed to 10 so that every unit has the same number and kind of components. For the variable structure setting, the depth of the tree randomly varies between 4 and 10, and components are sampled with replacement. For compositional generalization, an equal number of trees are generated for every module combination from 2 to 10. For parallel composition, the potential outcome is simulated for each component for each treatment as a function of input features and treatment. For sequential and hierarchical composition, the potential outcome is a function of input features, treatment, and potential outcomes of the parent components.

K.2 Models and Baseline implementation

1. *Hierarchical composition models*: Each distinct component in a structured unit is implemented as a separate MLP module with a hidden dimension size = $2 * \text{input_size}$ and batch size = 64 for each component. Models were trained using Adam optimizer with a learning rate of 0.01 (and adaptive cosine learning rate schedule with a starting learning rate of 0.001 for certain data sets). The total mean squared loss for all the component outcomes was optimized for the observed fine-grained outcomes of the hierarchical model. In contrast, loss for only unit-level potential outcomes was optimized for the unobserved fine-grained outcomes model. For the unobserved fine-grained outcomes model, the outcomes are passed hierarchically through the component interaction graph G_i as illustrated in Figure 1(c).
2. *Additive parallel composition models*: We implement an additive parallel model using two model classes: `random_forest` and `neural_network`. The differences between hierarchical and additive parallel composition models are as follows: (1) In parallel composition, the outcomes of each component are computed independently and not shared hierarchically. Second, an additive aggregation function is assumed, i.e., the unit-level outcome is the sum of the component’s outcomes. A three-layer, fully connected MLP architecture is used for neural network models with hidden layer dimension = 64 and ReLU activations. Models were trained using Adam optimizer with a learning rate of 0.01. For unobserved component-level outcomes, a mixture of experts (MoE) architecture [Jacobs et al., 1991, Shazeer et al., 2016] is used where each expert receives the high-dimensional covariates $\mathbf{X} \in \mathbb{R}^d$, initialized with the same number of experts as a number of distinct modules in the domain. We use a simple addition of the experts’ outcomes for the gating mechanism, as our data sets satisfy additive composition. For unobserved component-level covariates, entire unit-level covariates are passed to each component model to learn component-specific representations as part of learning component outcome functions.

Baselines: X-learner and non-parametric double machine learning implementation is from Econml library and random forests were used as the base models. TNet [Curth and Van der Schaar, 2021] implementation is taken from the GitHub repository catenets.

L Additional Results

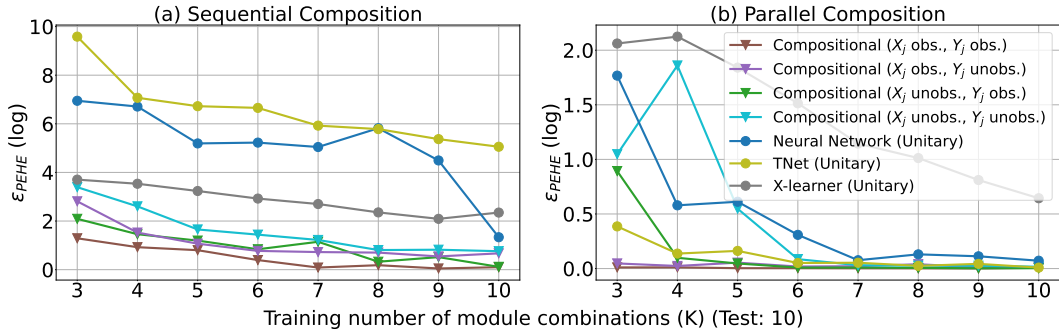


Figure 13: **Role of component-level data access and composition structure in the performance of compositional models:** PEHE error (in log) for models evaluated on compositional generalization task with varying degrees of component-level data access. (Lower is better). We observe that end-to-end trained models incorporating just modular structure compositionally generalize as trained on more module combinations. Unitary models show compositional generalization for additive parallel composition but perform comparably only for in-distribution combinations ($K=10$) for sequential composition, except X-learner. Note that the number of training samples increases as training depth increases.

M Algorithms

M.0.1 Hierarchical Composition Model

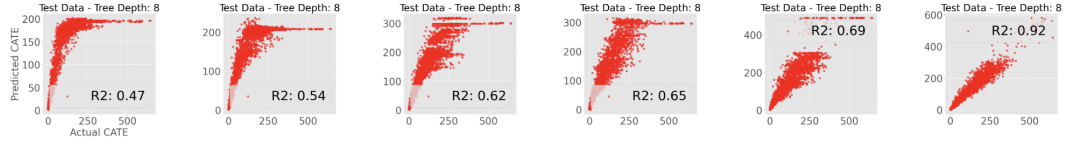


Figure 14: **Compositional generalization scatter plot for unitary model (X-learner):** This figure shows the scatter plot for test performance for the compositional generalization experiment. The training depths are varied from left to right $K = 3$ to 8 (left to right)

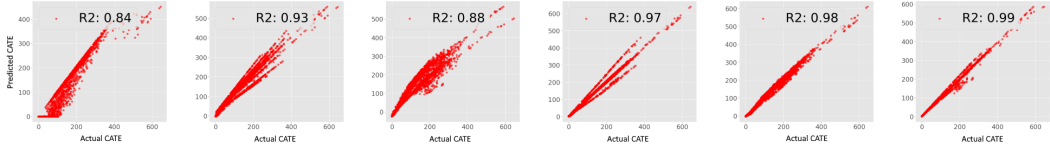


Figure 15: **Compositional generalization scatter plot for compositional model:** This figure shows the scatter plot for the predicted test performance of the compositional model on the test depth=8 when trained on increasing depths $K = 3$ to 8 (left to right).

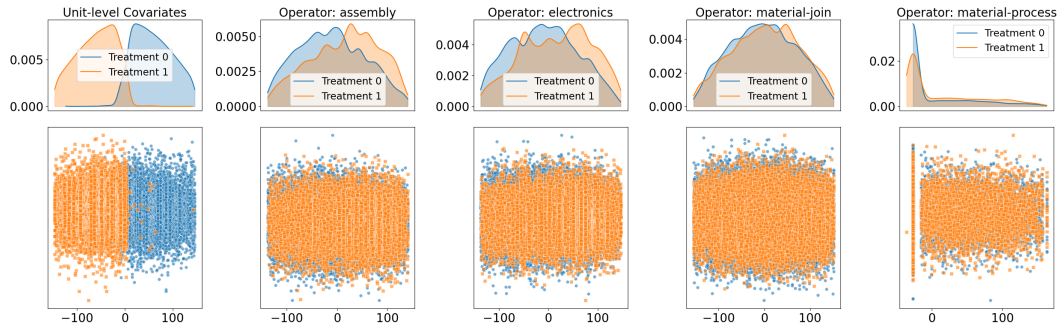


Figure 16: **Distribution mismatch due to structure-based treatment assignment for manufacturing data.** These density plots (top) and scatter plots (bottom) show the distribution mismatch between treatment and control groups at the unit level and component level. The plots are generated by first projecting the high-dimensional unit-level and component-level covariates to 1-dimensional using TSNE. The observational bias is created using tree_depth feature of the hierarchical structure.

Algorithm 1 Hierarchical Composition Model: Training

- 1: **Input:** Factual data set: $\mathcal{D}_F = \{q_i : \{\mathbf{x}_{ij}\}_{j=1:m_i}, t_i, y_i, \{y_{ij}\}_{j=1:m_i}\}_{i=1:n}$, number of distinct components k .
- 2: **Result:** Learned potential outcome models for each component: $\{\hat{f}_{\theta_1}, \hat{f}_{\theta_2}, \hat{f}_{\theta_3} \dots \hat{f}_{\theta_k}\}$
- 3: **while** not converged **do**
- 4: $loss_1, loss_2, loss_3, loss_k = 0$
- 5: **for** $i = 1$ **to** n **do**
- 6: Get the order of the components in which input is processed by using post-order traversal of the tree G_i .
- 7: $orderedList \leftarrow post_order_traversal(G_i)$
- 8: **for** component j in $orderedList$ **do**
- 9: $o \leftarrow component_class_index(j)$
- 10: // Potential outcome of a component depends on the potential outcome of the parent components according to graph G_i (assuming binary tree)
- 11: **if** component j has parents in G_i **then**
- 12: $\hat{y}_{ij} = \hat{f}_{\theta_o}(\mathbf{x}_{ij}, \{y_{l t_i}\}_{l \in Pa(c_j)}, t_i)$
- 13: **else if** component l does not have parents **then**
- 14: $\hat{y}_{ij} = \hat{f}_{\theta_o}(\mathbf{x}_{ij}, t_i)$
- 15: **end if**
- 16: $loss_o = loss_o + (\hat{y}_{ij} - y_{ij})^2$
- 17: **end for**
- 18: **end for**
- 19: Calculate gradients for the parameters for each module
- 20: **for** $o = 1$ **to** k **do**
- 21: $\delta_o \leftarrow \Delta_{\theta_o} \frac{1}{N_o} loss_o$
- 22: $\theta_o \leftarrow \theta_o - \alpha \delta_o$ independent training of all the component models.
- 23: **end for**
- 24: Check convergence criterion
- 25: **end while**

Algorithm 2 Hierarchical Composition Model: Inference

- 1: **Input:** Test data set: $\mathcal{D}_T = \{q_i : \{\mathbf{x}_{ij}\}_{j=1:m_i}\}_{i=1:n}$, learned potential outcome models for each component: $\{\hat{f}_{\theta_1}, \hat{f}_{\theta_2}, \hat{f}_{\theta_3} \dots \hat{f}_{\theta_k}\}$,
- 2: **Result:** CATESamples
- 3: **Procedure:**
- 4: $CATESamples \leftarrow \{\}$
- 5: **for** $i = 1$ **to** n **do**
- 6: Get the order of the operation in which input is processed by post-order traversal of the tree
- 7: $orderedList \leftarrow post_order_traversal(G_i)$
- 8: **for** component j in $orderedList$ **do**
- 9: $o \leftarrow component_class_index(j)$
- 10: **if** component j has parents in G_i **then**
- 11: $\hat{y}_{ij t_i} = \hat{f}_{\theta_o^*}(\mathbf{x}_{ij}, \{\hat{y}_{l t_i}\}_{l \in Pa(c_j)}, t_i)$
- 12: **else if** component l does not have parents **then**
- 13: $\hat{y}_{ij t_i} = \hat{f}_{\theta_o^*}(\mathbf{x}_{ij}, t_i)$
- 14: **end if**
- 15: **end for**
- 16: $\hat{\tau}(q_i) = \hat{y}_{im_i}(1) - \hat{y}_{im_i}(0)$, get the difference between estimated potential outcomes of the last component in G_i
- 17: $CATESamples \leftarrow CATESamples \cup \{(q_i, \hat{\tau}(q_i))\}$
- 18: **end for**

Algorithm 3 Additive Parallel Composition Model: Training

1: **Input:** Factual data set: $\mathcal{D}_F = \{q_i : \{\mathbf{x}_{ij}\}_{j=1:m_i}, t_i, y_i, \{y_{ij}\}_{j=1:m_i}\}_{i=1:n}$, number of distinct components k .
 2: **Result:** Learned potential outcome models for each component: $\{\hat{f}_{\theta_1}, \hat{f}_{\theta_2}, \hat{f}_{\theta_3} \dots \hat{f}_{\theta_k}\}$
 3: **Procedure:**
 4: $\mathcal{D}_1 \leftarrow \{\}, \mathcal{D}_2 \leftarrow \{\}, \mathcal{D}_3 \leftarrow \{\} \dots \mathcal{D}_k \leftarrow \{\}$
 5: **for** $i = 1$ **to** n **do**
 6: **for** $j = 1$ **to** m_i **do**
 7: $o \leftarrow \text{component_class_index}(j)$ index of distinct component class for j^{th} component instance.
 8: $\mathcal{D}_o \leftarrow \mathcal{D}_o \cup \{\mathbf{x}_{ij}, t_i, y_{ij}\}$
 9: **end for**
 10: **end for**
 11: **for** $o = 1$ **to** k **do**
 12: $N_o \leftarrow \text{len}(\mathcal{D}_o)$
 13: $\theta_o := \arg \min_{\theta} \frac{1}{N_o} \sum_{m=1}^{N_o} (\hat{f}_{\theta_o}(\mathbf{x}_m, t_m) - y_m)^2$ independent training of all the component models.
 14: **end for**

Algorithm 4 Additive Parallel Composition Model: Inference

1: **Input:** Test data set: $\mathcal{D}_{\mathcal{T}} = \{q_i : \{\mathbf{x}_{ij}\}_{j=1:m_i}\}_{i=1:n}$ and potential outcome models for each component: $\{\hat{f}_{\theta_1}, \hat{f}_{\theta_2}, \hat{f}_{\theta_3} \dots \hat{f}_{\theta_k}\}$,
 2: **Result:** CATESamples
 3: **Procedure:**
 4: $CATESamples \leftarrow \{\}$
 5: **for** $i = 1$ **to** n **do**
 6: **for** $j = 1$ **to** m_i **do**
 7: $o \leftarrow \text{component_class_index}(j)$
 8: $\hat{y}_{ij1} \leftarrow \hat{f}_{\theta_o^*}(\mathbf{x}_{ij}, 1)$
 9: $\hat{y}_{ij0} \leftarrow \hat{f}_{\theta_o^*}(\mathbf{x}_{ij}, 0)$
 10: **end for**
 11: $\hat{y}_{i1} = \sum_{j=1}^{m_i} \hat{y}_{ij1}$
 12: $\hat{y}_{i0} = \sum_{j=1}^{m_i} \hat{y}_{ij0}$
 13: $\hat{\tau}(q_i) = \hat{y}_{i1} - \hat{y}_{i0}$
 14: $CATESamples \leftarrow CATESamples \cup \{(q_i, \hat{\tau}(q_i))\}$
 15: **end for**
